Genetic dissection of aroma biosynthesis in melon and its relationship with climacteric ripening

Carlos Mayobre[1$], Lara Pereira[1,2$], Abdelali Eltahiri[1], Einat Bar[3], Efraim Lewinsohn[3], Jordi Garcia-Mas[1,4*], Marta Pujol[1,4*]

[1] Centre for Research in Agricultural Genomics (CRAG) CSIC-IRTA-UAB-UB, Edifici CRAG, Campus UAB, 08193 Bellaterra, Barcelona, Spain.

[2] *Present address*. Center for Applied Genetic Technologies, Genetics & Genomics, University of Georgia, Athens, GA 30602, U.S.

[3] Department of Vegetable Crops, Newe Ya'ar Research Center, Agricultural Research Organization, Volcani Center, Ramat Yishay, Israel

[4] Institut de Recerca i Tecnologia Agroalimentàries (IRTA), Edifici CRAG, Campus UAB, 08193 Bellaterra, Barcelona, Spain.

[$] These authors contributed equally to this work

[*]Corresponding authors addresses:

Jordi Garcia-Mas, jordi.garcia@irta.cat Phone: +34 935636600

Marta Pujol, marta.pujol@irta.cat Phone: +34 935636600

Highlights

- Two melon commercial varieties produced 88 different VOCs.
- Melon rind and flesh contributed differently to fruit aroma.
- *ETHQV8.1*, a climacteric ripening QTL, has an impact in the biosynthesis of VOCs.
- Candidate genes and QTLs have been identified as controlling VOCs production in melon.
- New tools for breeding fruit flavor in melon have been developed.

Abstract

Aroma is an essential trait in melon fruit quality, but its complexity and genetic basis is still poorly understood. The aim of this study was the identification of quantitative trait loci (QTLs) underlying volatile organic compounds (VOCs) biosynthesis in melon rind and flesh, using a Recombinant Inbred Line (RIL) population from the cross 'Piel de Sapo' (PS) x 'Védrantais' (VED), two commercial varieties segregating for ripening behavior. A total of 82 VOCs were detected by gas chromatography-mass spectrometry (GC-MS), and 166 QTLs were identified. The main QTL cluster was in chromosome 8, collocating with the previously described ripening-related QTL *ETHQV8.1*, with an important role in VOCs biosynthesis. QTL clusters involved in esters, lipid-derived volatiles and apocarotenoids were also identified, and candidate genes have been proposed for ethyl 3-(methylthio)propanoate and benzaldehyde biosynthesis. Our results provide genetic insides for deciphering fruit aroma in melon and offer new tools for flavor breeding.

Keywords: aroma, climacteric ripening, *Cucumis melo* L., GC-MS, QTL mapping, VOCs.

1. Introduction

Melon (*Cucumis melo* L.) is an important crop worldwide, with a global production of more than 27 million tonnes in 2018 (fao.org/faostat). Fruit quality is a complex trait determined by several fruit characteristics and is essential for consumer's appreciation. Melon is a very diverse species within the *Cucurbitaceae* family, comprising accessions that differ in color, texture, aroma, flavor and nutritional value (Pitrat, 2017). Melon is also an interesting crop to study fruit ripening, as the species includes climacteric and non-climacteric accessions. Climacteric ripening consists in a concomitant increase of the respiration rate and ethylene production at the onset of the ripening process, whereas in non-climacteric fruits both remain at a basal levels during ripening (Lelievre, Latche, Jones, Bouzayen, & Pech, 1997). Ethylene has a direct impact in aroma production (Manríquez et al., 2006; Shalit et al., 2001), which is one of the most important determinants of flavor and consumer preferences.

Fruit aroma depends on the concentration and the combination of volatile organic compounds (VOCs), which are genetically determined, but also highly influenced by environmental and post-harvest factors (Wyllie, Leach, Wang, & Shewfelt, 1994). More than 500 different VOCs have been identified in melon, and depending on the technique used more than 100 compounds can be found in a single accession (Esteras et al., 2018; Obando-Ulloa, Ruiz, Monforte, & Fernández-Trujillo, 2010; Pang et al., 2012). VOCs can originate from amino acids, fatty-acids or terpenes, and can be classified according to their chemical group. Esters, alcohols and aldehydes are the most abundant VOCs in melon, but other types of compounds such as benzenoids, ketones, furans, lactones, monoterpenes, sesquiterpenes or apocarotenoids are also found (Gonda et al., 2016). Each volatile has a different impact in the final aroma of the fruit depending on the individual odor threshold. Several melon accessions

have been studied combining gas chromatography-mass spectrometry (GC-MS) analyses with odor evaluations to determine the compounds that contribute the most to the unique flavor of melon varieties (Pang et al., 2012). Some key VOCs identified are nonanal, 6-nonenal (*Z*), 2,6-nonadienal-(*E,Z*), hexyl acetate, ethyl 2-methylpropanoate or phenylethyl alcohol. Each of these VOCs provides specific aroma and flavor to melon fruits, some of them being denominated as melon-like, cucumber-like, fruity, floral, sweet, green or even foul. For instance, most esters give fruity and sweet notes, whereas aldehydes and alcohols give green, fresh, cucumber-like notes (Gonda et al., 2016; Pang et al., 2012).

The volatile profile of climacteric and non-climacteric fruits differs both qualitative and quantitatively (Esteras et al., 2018; Moing et al., 2020; Obando-Ulloa et al., 2008). For instance, esters such as hexyl acetate and ethyl acetate are highly abundant in climacteric melons, whereas aldehydes like pentanal are more common in non-climacteric melons (Obando-Ulloa et al., 2008). Moreover, the diversity and amount of VOCs produced in climacteric melons is usually higher than in non-climacteric ones.

Melon is a diploid species (2n=2x=24) with a relatively small genome (357Mbp). The availability of a melon reference genome (Garcia-Mas et al., 2012), dense genetic maps (Pereira et al., 2018), germplasm collections and mapping populations such as Recombinant Inbred Lines (RILs) and Introgression Lines (ILs) have eased the identification of quantitative trait loci (QTLs) associated to fruit traits such as morphology, carotenoid content or ripening behavior (Obando-Ulloa et al., 2010; Pereira et al., 2018, 2020). RILs have shown to be powerful populations to detect QTLs in melon and other species as they usually present a high number of recombinations and represent diverse allelic combinations. Other powerful available tools in melon are databases such as Melonet-DB (Yano, Nonaka, & Ezura, 2018),

fruitENCODE (http://www.epigenome.cuhk.edu.hk/encode.html) and Melonomics (http://www.melonomics.net), which contain transcriptomic and epigenomic data, and the melon variome map (Zhao et al., 2019).

Biosynthesis pathways to several volatiles have been partially elucidated in melon although the complete biosynthetic pathways from amino acids, fatty acids and terpenes remain unknown. Aldehydes are hydrogenated to form alcohols (Manríquez et al., 2006), and alcohols are then acetylated to produce esters (Yahyaoui et al., 2002). The aminotransferases *CmBCAT1* and *CmArAT1* have been described to catalyze amino acids deamination, the first step of the production of several branched and sulfur VOCs (Gonda et al., 2010, 2013). In the phenylpropanoid pathway, *CmCNL* and *CmBAMT* participate in the synthesis of cinnamoyl-CoA and methyl benzoate, respectively (Gonda et al., 2018). In the fatty acid pathway, lipoxygenases (LOX), hydroperoxide lyases, isomerases and dehydrogenases play a role in the biosynthesis of C6 and C9 aliphatic aldehydes and alcohols from linoleic and linolenic acids (Schwab, Davidovich-Rikanati, & Lewinsohn, 2008). Several LOX genes have been identified in melon (Tang, Zhang, Cao, Wang, & Qi, 2015). For other aliphatic VOCs, α and β-oxidation have been proposed as possible biosynthetic pathways (Schwab et al., 2008). In the terpenoid pathway, the terpene synthases *CmTpsDul* and *CmTpsNY* modulate the accumulation of sesquiterpenes (Portnoy et al., 2008), whereas the cleavage dioxygenase *CmCCD1* cleaves carotenoids to produce several apocarotenoid VOCs such as geranylacetone and β-ionone (Ibdah et al., 2006).

In this study, we analyzed the volatile profile of a RIL population developed from a cross between two melon elite varieties, 'Piel de Sapo' (PS) and 'Védrantais' (VED) which segregates for many fruit quality traits, including aroma and ripening behavior (Pereira et al., 2020). QTL

mapping was performed using metabolite data obtained from both rind and flesh tissues, integrating phenotypic data from GC-MS and genotypic data previously obtained by genotyping by sequencing (Pereira et al., 2018). We hypothesize that both PS and VED may present functional alleles for the VOC synthesis, some of them related to ripening behavior. The aim of this work is to identify genetic factors controlling aroma production in melon which could be integrated into breeding programs for fruit flavor improvement.

2. Materials and methods

2.1. Plant material

The 89 RIL population, with 82 RILs in the F8 generation and seven in the F7, was developed from a cross between the non-aromatic '*Piel de Sapo'* T111 (PS) (*C. melo* ssp. *melo* group *inodorus*) and the aromatic '*Védrantais'* (VED) (*C. melo* ssp. *melo* group *cantalupensis,* French Charentais-type) by Pereira *et al.* (2018). The plants were grown at Caldes de Montbui (Barcelona) under greenhouse conditions, allowing only one melon per plant. The fruits were harvested at the ripe stage as previously defined (Pereira et al., 2018). The fruits analyzed in this study were harvested in summer 2015 (T3) and summer 2016 (T4 and T5), using a total of three biological replicates for the 89 RILs (one per harvest time) and 9 biological replicates for PS, VED and the hybrid PS x VED (three per harvest time) (Pereira et al., 2018).

2.2. Sample preparation for volatile extraction

Frozen samples of rind and flesh from the three biological replicates for each RIL were ground up and stored at -80 °C. All biological replicates were independently analyzed by GC-MS. Two grams of tissue were weighed and added to frozen chromatography 20 ml vials (Thermo Fisher Scientific®, Waltham, MA, U.S.) containing 7 ml of a saturated NaCl solution and 15 ppm of 3-

hexanone used as internal standard. Samples were sealed with silicone septa and stored at 4 °C in the dark for no longer than a week, until GC-MS analysis was performed.

2.3. Aroma analysis by GC-MS

Solid-Phase Micro-Extraction (SPME) was carried out using a 7890A gas chromatograph coupled to a 5975C mass spectrometer and a GC PAL 80 autosampler (Agilent Technologies®, Santa Clara, CA, U.S.). The chromatograph was equipped with an SPME fiber (50/30 µm DVB/CAR/PDMS, Merck®, Darmstadt, Germany) and a Sapiens-X5MS capillary column (30 m/0.25 mm/0.25 µm, Teknokroma®, Sant Cugat del Vallès, Spain). Samples were pre-incubated 15 min to 50 ºC at 250 rpm, and then the SPME fiber was exposed 30 min to the vial headspace. Sample injection was performed in splitless mode, starting at a temperature of 50 °C for 1 min, increasing 5 °C/min to 280 °C, and holding that temperature for 5 min (total time 52 min). The carrier gas was helium at a head pressure of 13.37 psi. The source temperature of the mass spectrometer was set at 230 °C and the quadrupole temperature at 150 °C, with no delay in the detection.

We performed an untargeted analysis for VOCs of rind and flesh samples. VOCs were identified by comparison of their mass spectra with the NIST 11 library (NIST/EPA/NIH) and by their Kovats retention index. The Kovats retention index was calculated using a mix of alkanes (C_7-C_{40} in hexane, Merck®, Darmstadt, Germany) under the same chromatographic conditions. We created a list of compounds identified in several samples by applying two quality criteria: a calculated Kovats index within a confidence interval of $\pm$10 comparing to tabulated standard values, and a minimum MS quality of 80. Compounds not matching both criteria were excluded from the analysis. For individual samples, when the proximity of two compounds lowered the MS quality, a cutoff of 50 was considered.

The content of each compound was estimated by comparison to the 3-hexanone internal standard peak area. Compounds were coded following a similar criterion to Freilich *et al.* (2015), grouping them based on their chemistry, tissue and name. Data was organized in four different subsets: each biological replicate individually and the mean of each line. Means were only considered when data of the three replicates was available. Medians of the biological replicates were also calculated.

Information about the odor of the compounds detected was extracted from the literature.

2.4. QTL analysis

QTL mapping was conducted with MapQTL 6® performing both interval mapping (IM) and the Kruskal-Wallis test (K-W). The genetic map used was described in Pereira et al. (2018) and was constructed using genotyping-by-sequencing data from the same RIL population. MapChart® was used for the map representation. For the statistical support of the QTL mapping, a permutation test with 1,000 iterations and 95% confidence was performed. QTLs with a LOD score ≥2.75 in at least one of the four subsets were preselected. The final map included only QTLs that reached the 2.75 threshold in the means subset, or a score ≥2.50 in two subsets. K-W scores were used to confirm the QTLs detected by IM. Candidate genes were selected using genome version v3.6.1 and according to functional annotation data from the Melonomics database v4.0 (https://www.melonomics.net/), orthologs found in PLAZA 4.0 (Van Bel et al., 2018) and transcriptomic data from the fruitENCODE database (http://www.epigenome.cuhk.edu.hk/encode.html).

2.5. Statistical analysis

The software R (v4.0.0) (https://www.r-project.org/) with the RStudio interface (v1.1.463) (http://www.rstudio.com/) was used to perform statistical analysis and to represent the data.

A Shapiro-Wilk test was performed to check the normality of the data and a correlation test was performed using the Spearman's rank correlation coefficient. Z scores were calculated to standardize the data since they deviated from normality. PCA was performed with "ggfortify", correlation was calculated with "Hmisc" and "corrplot" packages, and plots were generated with "gplots", "factoextra" and "ggplot2".

3. Results

3.1. General VOC analysis

Melon fruits from the RIL population produced 82 different VOCs, 79 were present in rind and all were present in flesh. According to their chemical structure, the list comprised 47 esters, 13 aldehydes, seven alcohols, six terpenes, four benzenoid derivatives, three ketones and two furans (Table 1). The distribution of all VOCs in the RIL population was not normal ($p<0.05$) but left-skewed. Both rind and flesh produced a great quantity of esters and aldehydes. Rind samples contained a higher quantity of these compounds compared to flesh (Supplementary Table S1-S4).

Table 1. VOCs identified by Kovats index and mass spectrum in the PS x VED RIL population.

	Compound	NIST nomenclature	Code[a]	RI[b]	CAS
Alcohols					
	2-Methylbutanol	1-Butanol, 2-methyl-	ALX_1B2M	729	137-32-6
	1-Hexanol		ALX_1HXO	864	111-27-3
	1-Octen-3-ol		ALX_1O3O	977	3391-86-4
	Benzyl Alcohol		ALX_BZOL	1034	100-51-6
	3-Octen-1-ol, (Z)-		ALX_3O1OZ	1066	20125-85-3
	1-Octanol		ALX_1OCOL	1069	111-87-5
	Phenylethyl Alcohol		ALX_PHEOL	1114	60-12-8
Aldehydes					
	3-Methylbutanal	Butanal, 3-methyl-	ADX_B3M	647	590-86-3
	2-Methylbutanal	Butanal, 2-methyl-	ADX_B2M	658	96-17-3
	Pentanal		ADX_PNL	695	110-62-3
	Hexanal		ADX_HXL	800	66-25-1
	Heptanal		ADX_HPL	901	111-71-7
	Benzaldehyde		ADX_BZALD	959	100-52-7
	Octanal		ADX_OCL	1002	124-13-0
	Benzeneacetaldehyde		ADX_BZACALD	1042	122-78-1

	2-Octenal, (E)-		ADX_2OLE	1063	2548-87-0
	6-Nonenal, (Z)-		ADX_6NNLZ	1103	2277-19-2
	Nonanal		ADX_NNL	1104	124-19-6
	2,6-Nonadienal, (E,Z)-		ADX_26NDLEZ	1152	557-48-2
	Decanal		ADX_DCL	1205	112-31-2
Benzenoids					
	Toluene		BX_TOL	761	108-88-3
	1,3-Dimethylbenzene	Benzene, 1,3-dimethyl-	BX_BZ13DM	862	108-38-3
	Styrene		BX_STYR	890	100-42-5
	1-Methoxy-4-methylbenzene	Benzene, 1-methoxy-4-methyl-	BX_BZ1M4M	1019	104-93-8
Esters					
	Ethyl Acetate		EX_EAC	615	141-78-6
	Ethyl propanoate	Propanoic acid, ethyl ester	EX_PEE	707	105-37-3
	n-Propyl acetate		EX_NPA	709	109-60-4
	Methyl butanoate	Butanoic acid, methyl ester	EX_BME	717	623-42-7
	Ethyl 2-methylpropanoate	Propanoic acid, 2-methyl-, ethyl ester	EX_P2MEE	751	97-62-1
	2-Methylpropyl acetate	Acetic acid, 2-methylpropyl ester	EX_A2MPE	767	110-19-0
	Methyl 2-methylbutanoate	Butanoic acid, 2-methyl-, methyl ester	EX_B2MME	772	868-57-5
	Ethyl butanoate	Butanoic acid, ethyl ester	EX_BEE	801	105-54-4
	Butyl acetate	Acetic acid, butyl ester	EX_ABE	812	123-86-4
	Ethyl 2-methylbutanoate	Butanoic acid, 2-methyl-, ethyl ester	EX_B2MEE	846	7452-79-1
	3-Methylbutyl acetate	1-Butanol, 3-methyl-, acetate	EX_1B3MA	873	123-92-2
	2-Methylbutyl acetate	1-Butanol, 2-methyl-, acetate	EX_1B2MA	877	624-41-9
	Propyl butanoate	Butanoic acid, propyl ester	EX_BPE	898	105-66-8
	Ethyl pentanoate	Pentanoic acid, ethyl ester	EX_PNEE	901	539-82-2
	Pentyl acetate	Acetic acid, pentyl ester	EX_APNE	913	628-63-7
	3-Methyl-2-buten-1-ol acetate	2-Buten-1-ol, 3-methyl-, acetate	EX_2B1O3MA	921	1191-16-8
	Methyl hexanoate	Hexanoic acid, methyl ester	EX_HXME	923	106-70-7
	Propyl 2-methylbutanoate	Butanoic acid, 2-methyl-, propyl ester	EX_B2M.PE	943	37064-20-3
	2-Methylpropyl butanoate	Butanoic acid, 2-methylpropyl ester	EX_B2MPE	953	539-90-2
	Ethyl (methylthio)acetate		EX_EMTHAC	983	4455-13-4
	Butyl butanoate	Butanoic acid, butyl ester	EX_BBE	995	109-21-7
	Ethyl hexanoate	Hexanoic acid, ethyl ester	EX_HXEE	1000	123-66-0
	3-Hexen-1-ol, acetate, (Z)-		EX_3HX1OAZ	1007	3681-71-8
	Hexyl acetate	Acetic acid, hexyl ester	EX_AHXE	1016	142-92-7
	1,2-Propanediol, diacetate		EX_12PLDA	1027	623-84-7
	Cyclohexyl acetate*	Acetic acid, cyclohexyl ester*	EX_ACHXE	1039	622-45-7
	2-Methylbutyl butanoate	Butanoic acid, 2-methylbutyl ester	EX_B2MBE	1057	51115-64-1
	2,3-Butanedioldiacetate		EX_23BOLDA	1061 & 1075	1114-92-7
	Ethyl 2,4-hexadienoate	2,4-Hexadienoic acid, ethyl ester	EX_24HXEE	1094	2396-84-1
	Propyl hexanoate	Hexanoic acid, propyl ester	EX_HXPE	1094	626-77-7
	Ethyl heptanoate	Heptanoic acid, ethyl ester	EX_HPEE	1098	106-30-9
	Ethyl 3-(methylthio)propanoate	3-(Methylthio)propanoic acid ethyl ester	EX_3MTHPEE	1100	13327-56-5
	Heptyl acetate	Acetic acid, heptyl ester	EX_AHPE	1112	112-06-1
	Ethyl (+-)-3-acetoxybutyrate*		EX_E3AXB	1114	27846-49-7
	1,3-Butanediol, diacetate		EX_13BOLDA	1128	1117-31-3
	2-Methylpropyl hexanoate	Hexanoic acid, 2-methylpropyl ester	EX_HX2MPE	1150	105-79-3
	Phenylmethyl acetate	Acetic acid, phenylmethyl ester	EX_APHME	1165	140-11-4
	Ethyl benzoate	Benzoic acid, ethyl ester	EX_BZEE	1171	93-89-0
	Diethyl butanedioate	Butanedioic acid, diethyl ester	EX_BDEE	1181	123-25-1
	Ethyl 4-octenoate	4-Octenoic acid, ethyl ester	EX_4OEE	1186	138234-61-4
	Butyl hexanoate	Hexanoic acid, butyl ester	EX_HXBE	1191	626-82-4
	Ethyl octanoate	Octanoic acid, ethyl ester	EX_OEE	1198	106-32-1
	Octyl acetate	Acetic acid, octyl ester	EX_AOE	1212	112-14-1
	Ethyl benzeneacetate	Benzeneacetic acid, ethyl ester	EX_BZAEE	1245	101-97-3
	2-Methylbutyl hexanoate	Hexanoic acid, 2-methylbutyl ester	EX_HX2MBE	1253	2601-13-0
	2-Phenylethyl acetate	Acetic acid, 2-phenylethyl ester	EX_A2PHEE	1257	103-45-7
	Ethyl decanoate	Decanoic acid, ethyl ester	EX_DCEE	1397	110-38-3
Furans					
	2-Ethylfuran	Furan, 2-ethyl-	FX_F2E	700	3208-16-0
	2-Pentylfuran	Furan, 2-pentyl-	FX_F2PN	992	3777-69-3

Ketones					
	2-Methyl-3-pentanone	3-Pentanone, 2-methyl-	KX_3PN2M	743	565-69-5
	4-Heptanone*		KX_4HPA	868	123-19-3
	6-Methyl-5-hepten-2-one	5-Hepten-2-one, 6-methyl-	KX_5HP2O	985	110-93-0
Terpenes					
	Eucalyptol		TX_EUL	1030	470-82-6
	β-Cylohomocitral		TX_ßCYHCL	1254	472-66-2
	Megastigma-4,6(Z),8(Z)-triene		TX_MEGA	1324	71186-25-9
	Caryophyllene		TX_ßCPHL	1421	87-44-5
	Cis-Geranylacetone		TX_CGERAC	1445	3879-26-3
	δ-Cadinene		TX_δCAD	1527	483-76-1

[a]X = R for rind, F for flesh

[b]RI = retention index

*Newly described in melon (to our knowledge)

We first analyzed the volatile profile of the parental lines. PS displayed a lower number of VOCs than VED in both rind (30 and 66, respectively) and flesh (27 and 71) tissues (Supplementary Table S1). The hybrid (Hyb) accumulated more compounds in rind (70) than in flesh (58). In all three lines, benzaldehyde was one of the most abundant compounds in rind, although the mean levels varied from 12914 ng g^{-1} of frozen tissue in PS to 56057 ng g^{-1} of frozen tissue in VED. VED and Hyb, both climacteric, also produced high amounts of the C6 lipid derived hexyl acetate (56132 ng g^{-1} and 38153 ng g^{-1} of frozen tissue, respectively). In flesh, lipid derived aldehydes such as nonanal (PS, 1364 ng g^{-1}) and octanal (Ved, 4220 ng g^{-1} and Hyb, 1530 ng g^{-1}) were predominant. The climacteric lines presented in addition high levels of ethyl hexanoate and butanoate derivatives in flesh. Some compounds were overproduced in Hyb fruits compared to PS and VED, such as heptanal and methyl hexanoate in rind, whereas other VOCs were underproduced like decanal in flesh.

VED produced significantly more esters, alcohols, aldehydes and terpenes than PS ($p<0.05$). For instance, VED samples produced 15 times more octanal and 40 times more benzyl alcohol in flesh, or 186 times more 2,3-butanedioldiacetate in rind. Furans and some ketones such as 2-ethylfuran and 2-methyl-3-pentanone were produced principally in PS fruits, whereas benzenoids were more abundant in Hyb rind. The total amount of VOCs in flesh was more

variable than in rind, possibly due to a stronger environmental effect in flesh samples caused by slight changes in ripening stage. VED main groups were esters (68-85 % in rind, 52-84 % in flesh), followed by aldehydes (12-27 % in rind, 4-38 % in flesh) and alcohols (2-5 % in rind, 2-14 % in flesh) (Supplemental Fig. S1). PS main groups were aldehydes (88-97 % in rind, 67-90 % in flesh), alcohols (1-3 % in rind, 1-4 % in flesh) and ketones (1 % in rind, 2-20 % in flesh). Hyb melons had an intermediate phenotype between PS and VED but were more similar to the VED profile.

The RIL population showed a left-skewed distribution and transgressive segregation for most compounds. Interestingly, flesh was the only tissue to produce β-cyclocitral, cis-geranylacetone and megastigma-4,6(*Z*),8(*Z*)-triene, the last one not being detected in any parental line. The only VOCs found in all samples were benzaldehyde in rind and eucalyptol in flesh, although nonanal and ethyl acetate were also produced by most lines in both tissues. Ethyl decanoate in rind and pentanal in flesh were rare in the population, detected only in one and 5 lines, respectively.

Correlations between VOCs in the RIL population were represented in a heatmap for both tissues, rind and flesh (Fig. 1). Esters were positively correlated among them, forming two clusters in flesh and 3 in rind. The cluster showing the strongest correlation comprised ethyl esters. Another ester cluster included also some alcohols such as hexanol, 2-methylbutanol and octanol, as well as eucalyptol in flesh and nonanal and decanal in rind. In addition, we found clusters of positive correlation for aldehydes, phenylalanine derived and lipid derived VOCs in rind, for acetates, nonanal derived VOCs and terpenes in flesh, plus some others with diverse composition. Furans, ketones and benzenoids showed negative correlation with the rest of the compounds.

3.2. QTL mapping

We found 166 QTLs for 63 different compounds, 77 of these QTLs were found in flesh and 89 in rind. Among them, 13 QTLs were coincident between tissues. All QTLs were confirmed by both IM and K-W, except QTL *EF_3MTHPEE_3.1* that did not fit the IM thresholds but had a significant K-W value. QTLs were identified in all 12 melon chromosomes (Fig. 2 and Table 2). Of the total number of QTLs, 18 were found in all four analyzed subsets (individual replicates and mean), 28 were detected in three subsets, and 4 were detected in two subsets but not in the mean subset. In addition, 72 QTLs appeared in only one subset and in the mean, and 44 were only found in the mean subset. The physical interval of the QTLs ranged from 5.9 Kb to 25.3 Mb, with a median of 9.2 cM and 1.96 Mb in genetic and physical distance, respectively. The median number of genes within these intervals was 173. We defined 12 clusters of QTLS which included multiple overlapping QTLs for compounds chemically similar and/or belonging to the same biochemical pathway (Table 2 and Supplementary Table S5). One of them on Chr08 contained up to 92 different QTLs.

Table 2. QTLs detected in the PS x VED RIL population.

Chr	C[a]	QTL	Genetic position (cM)	Nearest marker[b]	Size (Mb)[b]	LOD mean[c]	LOD T3[c]	LOD T4[c]	LOD T5[c]	K-W value	% Exp	Positive additive effect
1		*EF_E3AXB_1.1*	3.3	chr01_452338	1.2	**2.54**	0.79	**2.53**	1.35	<0.005	16.9	PS
		EF_NPA_1.1	122.2	chr01_36593213	0.7	**2.75**	1.66	1.30	1.31	<0.001	18.2	Ved
2		*ER_BME_2.1*	23.7	chr02_1937609	1.1	**2.55**	0.82	2.20	**3.33**	<0.005	16.7	PS
		EF_B2MME_2.1	50.8	chr02_6015657	3.7	**2.64**	0.77	**2.82**	1.31	<0.005	14.6	PS
	C2	*ER_1B2MA_2.1*	66.4	chr02_13326331	9.8	**3.04**	0.62	1.91	2.08	<0.005	19.7	PS
	C2	*ER_B2MME_2.1*	61.5	chr02_9079639	5.5	**3.08**	1.95	2.07	2.06	<0.005	19.9	PS
	C2	*EF_B2MME_2.2*	61.5	chr02_9079629	5.0	**2.79**	0.48	**3.02**	2.05	<0.0005	15.6	PS
	C2	*EF_B2M.PE_2.1*	64.8	chr02_11199109	5.0	**2.54**	0.95	0.99	**2.92**	<0.005	17.0	PS
	C2	*ER_B2MBE_2.1*	61.5	chr02_9079639	7.4	**2.85**	0.28	0.48	**2.97**	<0.0005	18.5	PS
		ADR_BZACALD_2.1	67.5	chr02_13326331	7.4	**2.76**	0.42	1.37	2.14	<0.001	18.0	PS
3		*ALR_1HXO_3.1*	38.9	chr03_6150294	4.5	**2.78**	**3.90**	0.94	1.26	<0.0001	18.1	PS
		FR_F2E_3.1	119.0	chr03_30900408	1.8	**2.87**	0.79	0.75	0.04	<0.0001	18.7	PS
	C3	*EF_EMTHAC_3.1*	119.6	chr03_30962715	0.4	**3.99**	1.51	1.82	**3.02**	<0.0001	24.0	Ved
	C3	*EF_3MTHPEE_3.1*	119.6	chr03_30962715	0.7	**2.64**	1.77	1.91	1.20	<0.0005	16.6	Ved

4		*EF_A2MPE_4.1*	4.9	chr04_1127842	0.8	**3.05**	1.56	0.55	1.65	<0.0005	18.9	Ved
		ER_NPA_4.1	68.4	chr04_15256396	3.1	**2.70**	**3.03**	1.00	0.90	<0.005	17.7	PS
		ADR_BZALD_4.1	72.4	chr04_15922403	0.9	**3.74**	**3.95**	1.71	1.54	<0.0001	23.6	PS
		KF_3PN2M_4.1	75.0	chr04_16687925	1.5	**2.90**	2.12	0.96	1.70	<0.001	19.1	Ved
	C4	*EF_EMTHAC_4.1*	75.0	chr04_16687925	3.0	**2.80**	0.94	1.29	**3.07**	<0.005	17.5	PS
	C4	*ER_B2MME_4.1*	75.0	chr04_16687925	1.5	**3.20**	2.32	2.09	1.82	<0.005	20.5	PS
	C4	*ER_3MTHPEE_4.1*	75.0	chr04_16687925	3.0	**2.96**	2.15	2.11	1.32	<0.0005	19.2	PS
		ER_NPA_4.2	86.7	chr04_20479692	1.8	**2.75**	1.37	1.17	1.88	<0.005	18.0	PS
		ER_A2MPE_4.1	92.7	chr04_25893667	6.0	**2.99**	0.36	1.36	2.12	<0.005	19.3	PS
5	C5.1	*ADF_BZALD_5.1*	0.0	chr05_182820	0.5	**2.86**	1.77	1.29	**3.91**	<0.0001	17.9	PS
	C5.1	*ALF_BZOL_5.1*	1.0	chr05_182820	0.5	**4.28**	**3.27**	**3.21**	**3.23**	<0.0001	20.6	PS
		EF_NPA_5.1	6.5	chr05_729528	1.2	**2.51**	**2.99**	1.84	0.37	<0.005	16.9	PS
	C5.2	*ALF_1B2M_5.1*	10.9	chr05_1085286	0.6	**2.55**	**2.80**	1.43	0.85	<0.005	17.0	PS
	C5.2	*ALR_1B2M_5.1*	12.5	chr05_1085286	0.6	**3.39**	**4.16**	0.50	1.46	<0.0005	21.6	PS
		ER_NPA_5.1	8.9	chr05_911334	0.5	**2.71**	**3.70**	0.80	1.51	<0.0005	17.7	PS
	C5.3	*ADF_NNL_5.1*	41.2	chr05_2516188	0.5	**3.80**	2.08	1.34	0.92	<0.0005	24.3	PS
	C5.3	*ADF_NNL_5.3*	48.2	chr05_2846615	1.7	**3.51**	1.92	0.56	1.79	<0.001	24.3	PS
	C5.3	*ADF_NNL_5.2*	44.6	chr05_2849664	0.0	**4.11**	1.95	1.32	1.29	<0.0005	25.9	PS
		EF_BEE_5.1	93.6	chr05_25326402	0.9	**2.74**	**2.91**	1.09	1.88	<0.001	17.2	Ved
6	C6.1	*ALR_3O1OZ_6.1*	21.7	chr06_2396961	1.8	**2.83**	2.42	2.03	1.16	<0.0001	18.7	Ved
	C6.1	*ER_3HX1OAZ_6.1*	21.7	chr06_2396961	0.2	**3.21**	**7.05**	1.34	**3.39**	<0.0001	20.9	Ved
	C6.1	*EF_3HX1OAZ_6.1*	28.0	chr06_3059995	1.3	**5.10**	**3.31**	**3.03**	**2.74**	<0.0001	29.6	Ved
	C6.1	*ER_3HX1OAZ_6.2*	28.0	chr06_3059995	0.9	**3.41**	**7.21**	1.47	**3.98**	<0.0001	22.1	Ved
	C6.2	*ALR_1B2M_6.1*	143.3	chr06_34012274	0.8	**3.29**	1.34	0.82	1.52	<0.0005	21.1	Ved
	C6.2	*ALF_BZOL_6.1*	144.3	chr06_34012274	1.1	**2.77**	0.54	0.72	**2.90**	<0.005	18.4	Ved
7		*EF_NPA_7.1*	3.0	chr07_551647	1.1	**2.76**	0.63	**3.21**	1.10	<0.005	16.5	Ved
		ER_BBE_7.1	14.3	chr07_1055303	0.6	**2.77**	1.19	1.49	0.26	<0.005	18.1	Ved
		TF_βCYHCL_7.1	56.1	chr07_18142671	18.7	**2.89**	0.03	2.37	2.14	<0.0005	18.0	Ved
8		*ER_24HXEE_8.2*	102.7	chr08_29813774	25.3	2.47	**3.02**	2.17	**2.77**	<0.001	16.3	Ved
		ADR_B3M_8.1	84.2	chr08_9446475	3.1	**2.59**	**3.44**	2.12	0.81	<0.0001	17.0	Ved
		EF_B2M.PE_8.2	90.3	chr08_24466782	18.5	**2.84**	**2.55**	1.07	0.47	<0.0005	18.7	Ved
		ER_AOE_8.1	84.2	chr08_9446475	0.8	**3.24**	**3.18**	**2.52**	1.59	<0.0001	20.8	Ved
	M_8.1	*ER_AHPE_8.1*	85.2	chr08_9634968	1.1	**3.13**	**3.63**	2.19	**2.81**	<0.0001	20.2	Ved
	M_8.1	*ER_ABE_8.1*	86.2	chr08_9634968	1.1	**3.81**	0.42	**2.70**	**2.73**	<0.0001	24.0	Ved
	M_8.1	*EF_B2M.PE_8.1*	86.5	chr08_9745430	8.2	**3.91**	**2.80**	1.54	1.09	<0.0005	24.8	Ved
	M_8.1	*ER_B2M.PE_8.1*	86.5	chr08_9634968	1.1	**3.36**	**2.74**	1.39	0.48	<0.0001	21.5	Ved
		EF_3MTHPEE_8.2	90.3	chr08_24466782	16.6	**3.83**	1.84	1.80	2.10	<0.0001	32.7	Ved
	M_8.2	*EF_24HXEE_8.1*	87.5	chr08_9941727	18.3	**2.53**	**3.50**	0.43	0.91	<0.0001	15.9	Ved
	M_8.2	*ER_ABE_8.2*	90.3	chr08_24466782	18.3	**3.26**	1.00	1.86	**2.65**	<0.0001	20.9	Ved
	M_8.2	*ALF_PHEOL_8.2*	91.3	chr08_24466782	18.3	**4.74**	**3.61**	1.22	**3.18**	<0.0001	27.8	Ved
		ER_23BOLDA_8.1	87.6	chr08_9941727	20.3	**2.82**	2.03	**3.65**	2.12	<0.0001	18.3	Ved
	M_8.3	*TR_EUL_8.1*	86.2	chr08_9634968	0.5	**6.70**	**7.53**	**3.52**	0.12	<0.0001	38.3	Ved
	M_8.3	*ALF_PHEOL_8.1*	86.5	chr08_9634968	0.5	**6.71**	**2.86**	1.65	**4.32**	<0.0001	37.0	Ved
	M_8.3	*EF_HXME_8.1*	86.5	chr08_9634968	0.5	**5.32**	**3.95**	**2.60**	1.09	<0.0001	30.6	Ved
	M_8.3	*ADR_OCL_8.1*	86.5	chr08_9634968	0.5	**4.26**	**3.40**	2.12	1.77	<0.0001	26.4	Ved

	ALR_OCOL_8.1	86.5	chr08_9634968	0.5	**4.17**	**4.28**	**3.86**	1.34	<0.0001	25.9	Ved
	ALR_1HXO_8.1	86.5	chr08_9634968	0.5	**3.87**	1.37	**3.33**	**2.57**	<0.0005	24.3	Ved
M_8.4	*EF_3MTHPEE_8.1*	86.5	chr08_9634968	0.8	**5.76**	**2.57**	**3.20**	**3.61**	<0.0001	32.7	Ved
	ER_EMTHAC_8.1	86.5	chr08_9634968	0.8	**5.05**	**4.71**	**4.63**	**3.40**	<0.0001	30.5	Ved
	ER_BZAEE_8.1	86.5	chr08_9634968	0.8	**4.95**	**4.44**	**3.58**	**5.19**	<0.0001	30.0	Ved
	ER_B2MME_8.1	86.5	chr08_9634968	0.8	**4.93**	**3.44**	**3.50**	**4.05**	<0.0001	29.9	Ved
	ADR_DCL_8.1	86.5	chr08_9634968	0.8	**4.79**	**3.29**	**3.11**	**4.45**	<0.0001	29.2	Ved
	ER_3MTHPEE_8.1	86.5	chr08_9634968	0.8	**4.64**	2.41	**3.68**	**3.54**	<0.0001	28.4	Ved
	BR_STYR_8.1	86.5	chr08_9634968	0.8	**3.73**	0.15	**3.50**	1.90	<0.0005	23.9	Ved
	ADR_BZACALD_8.1	86.5	chr08_9634968	0.8	**3.70**	**4.66**	**2.65**	**2.95**	<0.0001	23.4	Ved
	ADR_NNL_8.1	86.5	chr08_9634968	0.8	**3.68**	**2.78**	**2.58**	**2.75**	<0.0001	23.2	Ved
	ER_AHXE_8.1	86.5	chr08_9634968	0.8	**3.38**	2.08	2.05	**3.02**	<0.0001	21.6	Ved
	ER_A2PHEE_8.1	86.5	chr08_9634968	0.8	**2.60**	0.74	2.44	**2.75**	<0.0001	17.0	Ved
	ER_E3AXB_8.1	87.5	chr08_9941727	0.8	**4.29**	**2.70**	**2.61**	**3.37**	<0.0001	26.6	Ved
	KR_4HPA_8.1	87.5	chr08_24466782	0.8	0.21	0.18	**3.22**	**5.50**	<0.0001	1.5	PS
	EF_BZAEE_8.1	86.5	chr08_9634968	7.8	**4.31**	**2.70**	1.60	0.88	<0.0001	25.6	Ved
	ALF_1B2M_8.1	87.5	chr08_9941727	12.3	**4.09**	**3.68**	**2.77**	1.41	<0.0001	25.8	Ved
	KF_3PN2M_8.1	88.6	chr08_10225136	15.0	**3.03**	1.33	2.45	0.85	<0.001	19.8	PS
M_8.5	*EF_1B2MA_8.1*	86.5	chr08_9634968	16.3	**3.68**	1.91	2.46	1.98	<0.0001	22.3	Ved
	ER_24HXEE_8.1	86.5	chr08_9634968	16.3	**3.30**	**3.51**	**2.98**	**4.06**	<0.0005	21.1	Ved
	ER_HXEE_8.1	87.5	chr08_9941727	16.3	**4.26**	**5.58**	**3.98**	**3.69**	<0.0001	26.4	Ved
	EF_HXBE_8.1	87.5	chr08_9745430	16.3	**3.07**	**2.50**	1.37	0.77	<0.0001	20.1	Ved
	EF_BBE_8.1	88.6	chr08_10225136	16.3	**3.78**	1.65	1.40	2.06	<0.0001	24.1	Ved
	ER_B2MEE_8.1	88.9	chr08_10225136	16.3	**4.58**	**2.68**	1.93	**5.67**	<0.0001	28.1	Ved
	ALF_1HXO_8.1	88.9	chr08_10225136	16.3	**2.50**	2.19	**3.79**	0.08	<0.0001	15.8	Ved
	ER_BEE_8.1	90.3	chr08_24466782	16.3	**4.96**	1.93	**3.94**	**5.68**	<0.0001	30.0	Ved
	ER_PNEE_8.1	90.3	chr08_24466782	16.3	**4.92**	**4.23**	**3.06**	**2.99**	<0.0001	29.8	Ved
	ER_E3AXB_8.2	90.3	chr08_24466782	16.3	**3.28**	2.37	1.36	**3.10**	<0.0001	21.0	Ved
M_8.6	*ER_HXME_8.1*	86.5	chr08_9634968	18.0	**4.03**	**6.51**	**4.57**	0.04	<0.0001	25.2	Ved
	EF_HXPE_8.1	86.5	chr08_9745430	18.0	**2.79**	**3.15**	1.27	0.95	<0.0001	18.4	Ved
	EF_HX2MBE_8.1	88.6	chr08_10225136	18.0	**3.56**	2.29	1.63	0.91	<0.0001	22.9	Ved
	ER_HPEE_8.1	90.3	chr08_24466782	18.0	**3.35**	**2.88**	2.44	2.38	<0.0001	21.4	Ved
	BR_STYR_8.2	90.3	chr08_24466782	18.0	**2.85**	1.02	**2.97**	1.16	<0.001	18.8	Ved
	ER_OEE_8.1	90.3	chr08_24466782	18.0	**2.64**	1.68	1.62	**2.91**	<0.0001	17.3	Ved
	ER_B2MME_8.2	91.3	chr08_25723466	18.0	**4.25**	**3.50**	2.24	**4.00**	<0.0001	26.3	Ved
M_8.7	*EF_HPEE_8.1*	88.9	chr08_10225136	20.0	**4.02**	**3.40**	1.58	1.68	<0.0001	25.4	Ved
	EF_HX2MPE_8.1	90.3	chr08_24466782	20.0	**2.88**	1.82	1.11	1.15	<0.0001	19.0	Ved
	ALR_OCOL_8.2	90.3	chr08_24466782	20.0	1.44	**4.53**	**3.19**	0.08	<0.0001	9.8	Ved
	EF_DCEE_8.1	93.5	chr08_27430936	20.0	**3.09**	1.22	2.19	1.20	<0.0001	19.1	Ved
M_8.8	*EF_HPEE_8.2*	103.0	chr08_29813774	22.4	**3.31**	**3.40**	2.29	1.60	<0.0001	21.5	Ved
	ALR_OCOL_8.3	103.0	chr08_29813774	22.4	1.26	**4.19**	**2.82**	0.03	<0.0001	8.7	Ved
M_8.9	*ER_PEE_8.1*	90.3	chr08_24466782	16.1	**4.02**	1.68	2.23	**3.18**	<0.0001	25.1	Ved
	EF_B2MEE_8.1	90.3	chr08_24466782	16.1	**3.96**	1.87	1.81	1.31	<0.0001	23.8	Ved

		ER_EAC_8.1	90.3	chr08_24466782	17.8	**3.89**	2.04	1.87	**4.22**	<0.0005	24.4	Ved
		EF_E3AXB_8.2	93.5	chr08_27430936	19.7	**4.23**	**3.38**	2.31	1.84	<0.0001	26.6	Ved
	M_8.10	*EF_E3AXB_8.1*	90.3	chr08_24466782	15.8	**4.93**	2.40	1.47	1.99	<0.0001	30.3	Ved
		EF_1B2MA_8.2	90.3	chr08_24466782	15.8	**4.07**	2.24	**2.87**	1.63	<0.0001	24.4	Ved
		EF_HXEE_8.1	96.6	chr08_27868043	19.5	**5.39**	**3.55**	**4.01**	**2.89**	<0.0001	31.0	Ved
	M_8.11	*EF_B2MPE_8.1*	88.9	chr08_17287431	19.9	**2.84**	1.44	1.87	0.95	<0.005	18.7	Ved
		BF_BZ13DM_8.1	96.6	chr08_27868043	19.9	**2.97**	2.02	1.60	2.33	<0.0005	18.5	PS
		EF_PNEE_8.1	97.6	chr08_27868043	21.4	**4.90**	**3.94**	**3.28**	**2.94**	<0.0001	28.6	Ved
		EF_BEE_8.1	91.3	chr08_24466782	22.5	**3.06**	1.21	2.38	1.79	<0.0005	19.0	Ved
		ADR_NNL_8.2	91.7	chr08_25723466	12.1	**2.53**	**3.24**	1.99	1.73	<0.001	16.6	Ved
		ER_A2MPE_8.1	100.7	chr08_29419309	8.0	**2.90**	1.90	1.30	1.19	<0.0005	18.8	Ved
		EF_HXME_8.2	95.6	chr08_27868043	5.0	**5.12**	**4.97**	2.38	1.40	<0.0001	29.7	Ved
		ADR_BZACALD_8.2	91.7	chr08_25723466	5.3	**2.65**	**3.98**	2.07	**3.23**	<0.0001	17.3	Ved
	M_8.12	*EF_BZAEE_8.2*	95.6	chr08_27868043	3.7	**5.03**	**5.53**	0.73	1.70	<0.0001	29.3	Ved
		ER_HXME_8.2	96.6	chr08_27868043	3.7	**2.87**	**7.77**	1.02	0.01	<0.0001	18.7	Ved
		ADF_OCL_8.1	102.7	chr08_29419309	6.2	**3.13**	**3.63**	**2.56**	1.10	<0.0001	20.4	Ved
		ER_ABE_8.3	100.7	chr08_29419309	2.4	**3.77**	1.65	1.65	1.86	<0.0001	23.8	Ved
		ER_AHXE_8.2	99.6	chr08_29419309	1.9	**2.77**	**3.56**	1.77	1.23	<0.0001	18.1	Ved
		ADR_BZACALD_8.3	100.7	chr08_29419309	1.9	**4.77**	**6.68**	2.41	**4.27**	<0.0001	29.1	Ved
		EF_1B2MA_8.3	100.7	chr08_29419309	1.9	**3.70**	**3.38**	**2.66**	1.23	<0.0001	22.4	Ved
	M_8.13	*TR_EUL_8.2*	100.7	chr08_29419309	1.9	**3.31**	**4.71**	1.51	0.00	<0.0005	21.2	Ved
		EF_AHXE_8.1	100.7	chr08_29419309	1.9	**3.12**	2.10	1.95	0.88	<0.0001	19.3	Ved
		EF_B2M.PE_8.3	100.7	chr08_29419309	1.9	**3.01**	**3.16**	1.25	1.25	<0.005	19.7	Ved
		EF_APNE_8.1	100.7	chr08_29419309	1.9	**2.99**	**2.63**	2.02	1.06	<0.0001	18.6	Ved
		ER_PNEE_8.2	102.7	chr08_29813774	4.0	**4.14**	**4.50**	**2.70**	2.09	<0.0001	25.8	Ved
	M_8.14	*ER_HXEE_8.2*	102.7	chr08_29813774	4.0	**3.66**	**6.04**	**2.76**	2.36	<0.0001	23.2	Ved
		ER_HPEE_8.2	102.7	chr08_29813774	4.0	**3.30**	2.34	**2.76**	1.90	<0.0001	21.1	Ved
		ER_BZAEE_8.2	103.0	chr08_29813774	4.0	**3.93**	**5.90**	**2.72**	**3.10**	<0.0001	24.7	Ved
	M_8.15	*EF_E3AXB_8.3*	103.0	chr08_29813774	2.5	**3.46**	**2.54**	0.85	**4.13**	<0.0005	22.3	Ved
		EF_BEE_8.2	104.5	chr08_31341018	2.5	**4.26**	0.86	**5.01**	**3.73**	<0.0005	25.4	Ved
		EF_BZAEE_8.3	113.8	chr08_32190395	0.4	**3.90**	2.44	0.96	1.33	<0.0005	23.5	Ved
		EF_BEE_8.3	114.3	chr08_32190395	0.4	**4.50**	1.66	**4.24**	**3.90**	<0.0001	26.6	Ved
9		*ER_EAC_9.1*	52.9	chr09_20327236	1.7	**2.56**	**3.19**	0.49	1.17	<0.001	16.8	PS
		ER_BEE_9.1	64.3	chr09_21685526	2.3	**2.75**	1.74	1.02	1.31	<0.005	18.0	PS
		TF_CGERAC_9.1	65.3	chr09_21754707	0.6	**4.54**	**5.81**	**2.72**	**3.27**	<0.0001	26.8	Ved
	C9	*TF_βCYHCL_9.1*	62.6	chr09_21387823	0.7	**2.83**	0.91	2.00	**2.65**	<0.0001	17.7	Ved
		KF_5HP2O_9.1	64.3	chr09_21685526	0.5	**8.36**	**11.65**	**6.69**	**7.68**	<0.0001	45.7	Ved
10		*ER_PEE_10.1*	9.1	chr10_1133000	1.3	**2.52**	**3.17**	0.20	1.19	<0.005	16.6	PS
		ADF_HXL_10.1	31.0	chr10_3152004	2.4	**3.07**	0.61	0.17	**2.51**	<0.001	20.1	Ved
11		*BF_BZ13DM_11.1*	3.9	chr11_7689143	11.1	**4.82**	0.44	**3.17**	**2.86**	<0.0001	28.2	PS

C11.1	*ER_B2MME_11.1*	6.5	chr11_10453734	13.1	**2.83**	2.29	0.91	1.65	<0.0005	18.4	Ved
	ER_BEE_11.1	5.9	chr11_10453734	11.5	**3.54**	1.52	1.66	2.11	<0.0001	22.5	Ved
	EF_HXEE_11.1	5.9	chr11_10453734	11.5	**2.72**	1.21	**3.96**	1.32	<0.0005	17.0	Ved
	ER_PEE_11.1	6.5	chr11_10453734	11.2	**3.52**	2.47	1.91	1.25	<0.0005	22.4	Ved
	ER_EAC_11.1	6.5	chr11_10453734	11.2	**2.83**	1.51	1.49	1.08	<0.0005	18.4	Ved
C11.2	*EF_APNE_11.1*	88.3	chr11_32731899	1.2	**4.21**	1.07	2.06	**3.03**	<0.0001	25.1	PS
	EF_AHXE_11.1	88.3	chr11_32731899	1.2	**2.75**	0.27	1.83	**2.83**	<0.005	17.2	PS
	EF_1B2MA_11.1	88.3	chr11_32731899	1.3	**2.71**	0.98	1.93	**2.54**	<0.005	17.0	PS
	ER_BPE_11.1	88.5	chr11_32755551	1.3	**4.31**	1.76	1.38	**3.82**	<0.0001	26.7	PS
	ER_AHXE_11.1	88.5	chr11_32755551	1.3	**4.30**	1.76	1.60	**3.34**	<0.0005	26.6	PS
	ER_ABE_11.1	88.5	chr11_32755551	1.3	**3.97**	1.17	1.29	**2.68**	<0.0005	24.9	PS
	ER_1B2MA_11.1	88.5	chr11_32755551	1.6	**3.47**	2.02	1.56	1.81	<0.001	22.1	PS
	ER_12PLDA_11.1	88.5	chr11_32755551	1.9	**3.21**	**2.74**	0.35	1.14	<0.0001	20.6	PS
	ER_2B1O3MA_11.1	88.5	chr11_32755551	1.9	**3.05**	0.01	1.34	1.72	<0.005	19.7	PS
	ER_3HX1OAZ_11.1	90.5	chr11_32928874	2.0	**2.55**	1.51	0.98	**3.72**	<0.005	17.0	PS
	ER_APNE_11.1	88.5	chr11_32755551	0.6	**4.30**	1.59	1.92	**3.00**	<0.001	26.6	PS
	ER_BBE_11.1	88.5	chr11_32755551	1.1	**2.73**	0.31	0.69	**3.43**	<0.0005	17.9	PS
	EF_12PLDA_11.1	91.5	chr11_32928874	1.2	**2.72**	**3.30**	0.39	0.30	<0.0005	18.0	PS
	EF_3HX1OAZ_11.1	107.8	chr11_34107169	0.6	**3.51**	1.53	1.82	2.39	<0.0001	21.4	PS
12	*FR_F2PN_12.1*	0.0	chr12_399410	1.1	**3.26**	**2.51**	1.18	**2.50**	<0.0005	21.2	PS
	FR_F2PN_12.2	19.0	chr00_4930997	1.5	**4.33**	0.70	0.66	**4.51**	<0.0001	27.1	PS
	ALF_1B2M_12.1	94.0	chr12_25861436	0.7	**2.52**	**3.28**	1.08	2.34	<0.005	20.3	PS
	EF_PEE_12.1	96.2	chr12_26103502	0.4	**3.80**	1.33	**2.69**	2.22	<0.0001	24.2	PS
	EF_BZEE_12.1	99.6	chr12_26757080	1.3	**2.76**	0.79	1.32	1.25	<0.005	17.3	PS

[a] C = cluster, M = merged

[b] Physical positions and distances refer to the v3.6.1 melon reference genome

[c] LOD ≥2.50 are in bold, LOD ≥2.75 are underlined

The highest LOD values were found in clusters on Chr06, Chr08 and Chr09. On Chr06, we detected a stable QTL cluster (C6.1) with a LOD score of 7.21 related to lipid-derived VOCs, with three QTLs for 3-hexen-1-ol acetate (*Z*) at 19-32 cM in both flesh and rind, and one QTL for 3-octen-1-ol (*Z*) for rind. The narrowest QTL interval included 26 annotated genes and the positive additive effect of C6.1 was provided by the VED allele. The largest cluster was found on Chr08, formed by 92 QTLs overlapping between 71-121 cM. Many of these QTL were stable since they were detected in all subsets. We could identify 3 recurrent maximum LOD peaks, which were located around 86, 91 or 100 cM. These QTLs were merged (M) in black rectangles to help visualization (Fig. 2 and Table 2). The length of these QTLs ranged 0.41-25 Mb. The

positive effect was provided by the VED allele for all significant VOCs, except for 4-heptanone, 2-methyl-3-pentanone and 1,3-dimethylbenzene. QTLs in this cluster explained 15-30 % of the variation. Another QTL cluster (C9) was found on Chr09 in flesh tissue for two terpenes and a ketone derived from the carotenoid cleavage pathway. The cluster shares an interval of 0.51 Mb at 62-69 cM, a region that contains 73 annotated genes. The highest LOD value was 11.65 for 6-methyl-5-hepten-2-one and explained 45 % of the variance.

Other minor QTLs for compounds relevant for melon flavour were found on Chr02, Chr03, Chr05 and Chr11. On Chr02, we found a cluster of 5 QTLs (C2) with a LOD peak of 3.08 between 61,5-67,5 cM. C2 included QTLs for isoleucine-derived esters, the PS allele contributing to higher content of these VOCs. Another cluster (C3) was found at the end of Chr03, containing two methionine-derived sulfur esters and overlapping in 0.39 Mb (containing 59 genes), with a positive effect of the VED allele. The ethyl (methylthio)acetate QTL had a LOD above 3.00 in one of the subsets, whereas the QTL for ethyl 3-(methylthio)propanoate was significant only using K-W test. On Chr05, a cluster (C5.1) containing 109 genes was detected for benzaldehyde and benzyl alcohol, two phenylalanine derived VOCs. The benzyl alcohol QTL was detected in all subsets. Two more clusters were found on chromosome 5 (C5.2 and C5.3) for 1-butanol-2-methyl and nonanal. In all these QTLs the positive additive effect was provided by the PS allele. Two ester clusters were localized on Chr11, C11.1 and C11.2, containing predominantly ethyl esters and acetates, respectively. The first cluster, with a positive effect of the VED allele, was located between 0-11 cM and had a LOD peak of 3.54. The second cluster, with a positive additive effect of the PS allele, was detected at 81-100 cM and had a LOD peak of 4.31.

3.3. VOCs and ripening

The RIL population segregates for climacteric ripening, as expected since the two parental lines have opposite ripening behavior (Supplementary Table S2). The PS x VED RILs were classified in a previous work as climacteric, non-climacteric and “unstable-climacteric”, the last for those RILs that were climacteric only in some biological replicates (Pereira et al., 2020). We first compared the three groups by doing a PCA using the mean subset (Fig. 3). Non-climacteric RILs were grouped apart from the climacteric lines and showed less diversity, in both rind and flesh. Climacteric RILs, which produced a more diverse profile and a higher quantity of VOCs, presented higher dispersion. “Unstable-climacteric” RILs were distributed within the two other groups. The same pattern was observed when each individual replicate was analyzed (Supplementary Fig. S2). In rind tissue, the metabolites that represented the largest positive and negative effects for each principal component were 2-ethylfuran and hexyl acetate, respectively, in PC1 (X-axis), and ethyl octanoate and β-caryophyllene in PC2 (Y-axis). In flesh, PC1 was determined principally by 2-methylbutyl acetate and 2-methyl-3-pentanone, while PC2 was determined by 1-octen-3-ol and 2-methylpropyl butanoate.

The relative amount of each chemical group was calculated and compared between climacteric and non-climacteric RILs for each subset (Fig. 4). Due to the dispersion of “unstable-climacteric” lines in volatile content, they were excluded from the analysis. In climacteric lines, esters were predominant (45-80% rind, 75-90% flesh), followed by aldehydes (20-55% rind, 5-15% flesh). Non-climacteric lines had a more variable phenotype depending on the tissue. In rind, aldehydes were the main group (50-95%), followed by esters (5-45%), while in flesh both esters and aldehydes showed high and variable contents ranging from 20-90% for esters and 5-60% for aldehydes. Therefore, an enrichment of esters was observed in the flesh of non-climacteric RILs compared to rind tissue. Alcohols and the rest of the chemical groups showed similar mass percentages in climacteric and non-climacteric RILs.

4. Discussion

Aroma is one of the main determinants of melon flavor. Insights into the genetic control of VOC biosynthesis and regulation would facilitate its incorporation in breeding programs, leading to varieties with superior flavor and better consumer's acceptance. The composition of rind aroma has been neglected in some studies, despite its relevance for fruit quality and acceptability and divergent VOC profiling. In this study, we used PS and VED which are both elite commercial varieties with good flavor but differ in ripening behavior, fruit color and volatile profile, among other fruit traits.

4.1. Volatile profile

From the 82 VOCs detected, three had not been previously identified in melon, to our knowledge (Table 1). The number of VOCs found was in agreement with other GC-MS experiments in melon that used SPME fibers (Shi et al., 2020). We found compounds that had been previously described as key compounds for flavor in muskmelons and honeydews. For instance, 6-nonenal (*Z*) and nonanal, which give melon-like and citrus notes, and ethyl acetate, which evokes butterscotch (Kemp, Knavel, & Stoltz, 1972; Lignou, Parker, Oruna-Concha, & Mottram, 2013; Wyllie, Leach, Wang, & Shewfelt, 1995). Other compounds like 2-methylbutyl acetate, methyl 2-methylbutanoate, ethyl 2-methylpropanoate, hexyl acetate, ethyl butanoate and ethyl hexanoate, which were more abundant in VED melons, have been reported as important fruity, floral and sweet compounds (Lignou et al., 2013; Pang et al., 2012; Wyllie et al., 1995). Another key compound found in the population was 2,6-nonadienal (*E,Z*), which gives cucumber-like notes and is the main compound in honeydews (Perry, Wang,

337 & Lin, 2009). All the cited key VOCs were detected above its reported odor threshold,
338 suggesting that they play an important role in PS and VED final flavor.

339 Rind accumulated higher levels of VOCs, probably due to the lesser water content as
340 compared to flesh, and, remarkably, presented less variability than flesh tissues
341 (Supplementary Fig. S1 and Supplementary Table S1-2). The higher production of VOCs in VED
342 as compared to PS correlates with a more intense smell. Fruity aroma of VED melons comes
343 mainly from esters in both rind and flesh, in agreement with several studies that described
344 Cantaloupe aroma (Esteras, Rambla, Sánchez, Granell, & Picó, 2020; Esteras et al., 2018;
345 Obando-Ulloa et al., 2008). Conversely, the fresh aroma of PS comes from a high accumulation
346 of aldehydes, also shown in previous studies (Esteras et al., 2020, 2018; Obando-Ulloa et al.,
347 2008). Hyb melons also displayed many volatile compounds and had an intense fruity aroma,
348 likely conferred by high amounts of esters. The transgressive segregation showed for
349 heptanal, methyl hexanoate and decanal in Hyb melons exposed the effect of heterosis. The
350 volatile profile of the RILs was very diverse, although most lines were more similar to VED than
351 to PS, as the Hyb. Therefore, some VED alleles probably have a dominant effect on the final
352 volatile profile. A similar pattern was observed for climacteric ripening, which determines to
353 a high extent the volatile profile (Pereira et al., 2020).

354 Ethyl esters, acetates, and compounds coming from the same biosynthetic pathway were
355 positively correlated (Fig. 1). The ethyl ester correlation cluster could be explained by the
356 activity of alcohol acyltransferases able to transform several substrates (El-Sharkawy et al.,
357 2005; Yahyaoui et al., 2002). Another ester cluster including several alcohols could be related
358 to ethylene, as both alcohol dehydrogenases and acyltransferases are associated with
359 ethylene production (Manríquez et al., 2006; Shalit et al., 2001). The rest of correlation

clusters also grouped compounds from the same chemical group or the same biochemical origin, being probably led by the same key enzymes. For instance, hexanoate or nonanal derivatives are lipid derived VOCs (Schwab et al., 2008), β-caryophyllene and δ-cadinene are terpenoids, and 2-methylbutanal or benzene derivatives belong to isoleucine and phenylalanine pathways, respectively, through the *CmBCAT1* and *CmArAT1* enzymes (Gonda et al., 2010). The inverse correlation of furans and certain benzenoids observed in PS, with most esters abundant in VED, could be explained by the different ripening behavior of both accessions.

4.2. QTL mapping

We found a similar number of QTLs (166) and segregating compounds (63) (Table 2 and Fig. 2) as Galpaz *et al.* (2018), which also used VOC profiling in a RIL population for QTL analysis (FDR<10 %, 145 QTLs for 58 different compounds in 99 RILs). The median length of the QTLs (9.2 cM and 1.96 Mb) is comparable with the 9.42 cM and 0.94 Mb obtained by Pereira *et al.* (2018) using the same population for other traits. The maximum percentage of variance explained by a QTL in our study was 45.7 %, near to a monogenic inheritance, but the majority ranged from 15-25 %, which suggests a complex inheritance in VOCs synthesis. Similar values have been reported in melon (Galpaz et al., 2018). Multiple QTLs on different chromosomes controlled the amount of certain compounds, also indicating multigenic inheritance.

An important environmental effect was observed in the volatile composition of RILs, as 72 QTLs were found only in one year. Despite the environmental effect, 30.12 % of the QTLs were detected in a minimum of two subsets. When using the mean subset, which should be more robust, we found consistent results for the QTLs detected in more than one subset. We

decided to focus on the most reliable QTLs detected at least in two subsets and in those forming clusters.

The detection of clusters of QTLs could be due to a common regulation, a common step in a biochemical pathway or an enzyme capable of transforming several substrates, as had been previously reported in melon (El-Sharkawy et al., 2005; Gonda et al., 2010). For instance, several isoleucine derived VOCs were controlled by the QTL cluster C2 on Chr02. The length of the confidence interval determined for each cluster was variable, ranging from 0.39 Mb to 22.44 Mb. Some of them contained 100 genes or less, such as the sulfur esters cluster on Chr03 and the benzaldehyde and benzoic acid cluster on Chr05.

4.2.1. Branched-chain amino acid aminotransferases as first-step enzymes in the volatile biosynthesis

The sulfur compounds ethyl(methylthio)acetate and ethyl 3-(methylthio)propanoate are important odorants giving grassy and earthy aromas (Wyllie et al., 1994). A QTL cluster modulating the production of these compounds was detected at the end of Chr03 partially overlapping with a 2-ethylfuran QTL. This cluster includes the previously described *CmBCAT1* gene (*MELO3C010776*) at 20-40 Kb from the maximum LOD peak. The aminotransferase *CmBCAT1* is involved in the first step of the L-leucine, L-isoleucine and L-valine catabolic pathways when expressed *in vitro* (Gonda et al., 2010). Previous studies in *Arabidopsis* have shown that *BCAT4*, a homologue of *CmBCAT1*, participates in the methionine elongation pathway (Schuster, Knill, Reichelt, Gershenzon, & Binder, 2006). Therefore, the melon enzyme may participate in the deamination of L-methionine to form the precursor of ethyl 3-(methylthio)propanoate. According to transcriptomic data from fruitENCODE (http://www.epigenome.cuhk.edu.hk/encode.html), *MELO3C010776* is highly expressed in

VED flesh compared to PS. The two sulfur compounds were only detected in VED, and interestingly, correlate with the ethylene production. Apart from *MELO3C010776*, an ethylene-responsive transcription factor and an ACC synthase are present in this interval and could also have an effect for this trait. In addition, this region overlaps with an aroma QTL described by Pereira *et al.* (2020), which could be related to the *CmBCAT1* activity.

A *BCAT-like* gene (*MELO3C003454*) was found in the *EF_A2MPE_4.1* interval on Chr04. 2-Methylpropyl acetate is an important odorant described by (Pang et al., 2012) and having a floral aroma. In the presence of valine, higher quantities of 2-methylpropyl acetate were produced (Gonda et al., 2010). This gene could have a similar activity to *CmBCAT1*. A BLAST search revealed that *MELO3C003454* is similar to predicted chloroplastic D-aminoacid aminotransferases in peach, strawberry and apple. Thus, a hypothetical activity of this enzyme could be the deamination of D-valine into the precursor of 2-methylpropanal. The gene underlying 2-methylbutanal derivatives' QTL cluster on Chr02 could also be an aminotransferase, but no annotated BCAT-encoding gene has been found within this interval.

4.2.2. Aldehyde oxidases and dehydrogenases

Benzaldehyde and benzyl alcohol are also important odorants in melon, having almond and floral-fruity aroma, respectively (Jordán, Shaw, & Goodner, 2001; Pang et al., 2012). These compounds were controlled by a QTL on Chr05 in flesh, which includes three aldehyde oxidases annotated less than 30 Kb downstream the maximum LOD peak. Although benzaldehyde is produced at high quantities in rind, these enzymes could also be important for flesh aroma. A BLAST analysis and a search for orthologues in PLAZA 4.0 (Van Bel et al., 2018) revealed that *MELO3C014719* is an indole-3-acetaldehyde oxidase-like and is similar to the *A. thaliana* AAO4 protein, which was reported to transform benzaldehyde into benzoic

acid in siliques (Ibdah, Chen, Wilkerson, & Pichersky, 2009). The transcriptomic data from fruitENCODE supports this idea, as *MELO3C014719* is more expressed in VED flesh than in PS. Both functional annotation and transcriptomic data point out *MELO3C014719* as a likely candidate gene.

We identified another candidate gene within the 2-methylbutanol QTL interval, also on Chr05. Although 2-methylbutanol is not a potent odorant, it is the precursor of 2-methylbutyl acetate, described by Wyllie *et al.* (1995) and Lignou et al. (2013) as a key compound in melon flavor giving banana and pear notes. *MELO3C014601*, an aldehyde dehydrogenase, could catalyze the dehydrogenation of 2-methylbutanal to 2-methylbutanoate, and therefore limiting the synthesis of the corresponding alcohol. However, the amount of alcohols and acids also depends on the activity of alcohol acyltransferases (El-Sharkawy et al., 2005). Functional validation would be needed to confirm this candidate gene.

4.2.3. Alcohol acyltransferases in ester formation

Ester synthesis is known to be driven by alcohol acyltransferases. The characterization of AAT1, AAT2, AAT3 and AAT4 showed their ability to transform a great variety of substrates (El-Sharkawy et al., 2005; Yahyaoui et al., 2002). These enzymes were described as key steps in the unique aroma of melon (Liu et al., 2020). AAT1, AAT2 and AAT3 are located within the first QTL cluster on Chr11 at 0-11.7 cM (C11.1). AAT1 is the most active enzyme and prefers C6 substrates, AAT3 prefers benzyl alcohol and acetate as substrates and AAT2 is inactive in VED (El-Sharkawy et al., 2005; Yahyaoui et al., 2002). Interestingly, ethyl acetate and ethyl propanoate were tested but not detected as products of these three enzymes (El-Sharkawy et al., 2005). Other AATs in the interval such as *MELO3C024764* and *MELO3C024769* may be involved in the synthesis of these compounds.

Within the QTL cluster on Chr11 at 81-100 cM (C11.2), some metabolic enzymes and transcription factors could be involved in the synthesis of esters, but no clear candidate gene could be identified. Due to the interest of ester compounds, a fine mapping of this region will be performed to help identifying possible candidates within the 234 genes contained in the cluster (Table 2).

4.2.4. Fatty-acid pathway

Fatty-acid-derived VOCs such as 2,6-nonadienal and 6-nonenal (*Z*), which give honeydew and cucumber notes, form part of the key VOCs identified in melon (Pang et al., 2012). Lipoxygenases increase their expression at the final stages of fruit ripening. These enzymes can also be enhanced by the addition of fatty acid precursors (Tang et al., 2015). On Chr05, *EF_BEE_5.1,* a QTL for ethyl butanoate, another relevant odorant with ripe melon aroma (Lignou et al., 2013), contains a cluster of 10 lipoxygenases and a γ-aminobutyrate transaminase that could be involved in the formation of the butanoate backbone. In the nonanal cluster C5.3, we identified 2 lipid-transfer proteins that could be involved in the first steps of the synthesis. On Chr06, the QTL cluster C6.1 for *ER/F_3HX1OAZ_6.1/2* and *ALR_3O1OZ_6.1* contains β-oxidation-related genes such as a 3-ketoacyl-CoA thiolase and a synthase (Goepfert & Poirier, 2007). These candidate genes have also been found within *ER_BBE_7.1* interval however its activity would need to be validated.

4.2.5. Carotenoid derivatives

Some terpenoids such as β-cyclocitral and 6-methyl-5-hepten-2-one are important odorants in melon, giving tropical-like and peculiar aromas (Gonda et al., 2016; Pang et al., 2012). Their biosynthesis starts from isopentenyl diphosphate (IPP) or dimethyl allyl diphosphate (DMAPP), which can form chains to create the precursors of mono-, sesquiterpenes and

carotenoids. Two terpene synthases in 'Dulce' and 'Noy Yizre'el' accessions have been already described in melon (Portnoy et al., 2008). Carotenoid cleavage dioxygenases such as CmCCD1 can cleave larger terpenes to generate VOCs such as geranylacetone, 6-methyl-5-hepten-2-one and ionone (Ibdah et al., 2006; Vogel, Tan, McCarty, & Klee, 2008). In our study, we found a QTL cluster with the highest LOD value for 6-methyl-5-hepten-2-one, and two other QTLs for geranylacetone and β-cyclohomocitral. All of them are apocarotenoids, and the positive additive effect is given by the VED allele. This QTL cluster is located on Chr09, and within its interval we found the *CmOr* gene, *MELO3C005449*, responsible for the orange flesh color (Tzuri et al., 2015). *CmOr* segregates in the RIL population, and we observed that only orange fleshed lines (Pereira et al., 2018) accumulated apocarotenoids. Thus, *CmOr* is likely the underlying gene for the apocarotenoid QTL cluster. This correlation between orange flesh color and the presence of apocarotenoids was also seen in previous studies (Esteras et al., 2018; Ibdah et al., 2006). A new QTL mapping including only the orange fleshed RILs did not reveal any new QTLs for those VOCs.

4.2.6. Aroma as an ethylene-dependent trait

The association between aroma profile and climacteric ripening in melon has been largely studied (Flores et al., 2002; Li et al., 2016; Obando-Ulloa et al., 2008; Pereira et al., 2020), since both the aroma and other traits associated to ripening have a major influence on fruit quality. The ethylene peak characteristic of climacteric ripening promotes ester and alcohol formation (El-Sharkawy et al., 2005; Li et al., 2016; Manríquez et al., 2006). Indeed, the presence of aroma has previously been used as a climacteric trait (Pereira et al., 2020).

As previously reported by Obando-Ulloa *et al.* (2008) and Esteras *et al.* (2018), we observed a predominance of esters in climacteric lines and aldehydes in non-climacteric lines (Fig. 4).

Moreover, esters were the principal components leading to the climacteric profile in the PCA (Fig. 3). The high diversity in the VOC profile of climacteric lines had also been seen when comparing climacteric and non-climacteric accessions (Esteras et al., 2018; Moing et al., 2020). We have also noticed that the balance between esters and aldehydes remains constant, summing up more than 90 % of the total amount of VOCs (Supplementary Table S2). This balance could be explained by the ethylene-dependent nature of alcohol dehydrogenases and alcohol acyltransferases (El-Sharkawy et al., 2005; Manríquez et al., 2006). Shi *et al.* (2020) classified 39 melon cultivars according to their aldehyde/ester ratio and observed that several cultivars had an intermediate phenotype. The evaluation of the aroma production in our RIL population provides nuances to the previous classification between climacteric and non-climacteric behavior, since some RILs classified as climacteric produce high levels of aldehydes and others classified as non-climacteric produce abundant esters (Supplementary Table S2). In addition, ester abundance was increased by PS alleles in Chr02 and Chr11. Esteras *et al.* (2018) also detected a climacteric-like profile, linked to esters, in some *inodorus* accessions. In fact, climacteric ripening is not an absolute trait, as it has been seen in the RIL population showing different degrees of ethylene production (Pereira et al., 2020).

Many of our QTL intervals contain ethylene-related transcription factors that could play a role in the production of VOCs. For instance, the cluster on Chr02 overlaps with ripening-related QTLs that were previously described, such as QTLs for abscission layer formation, firmness, ethylene production and earliness of aroma (Pereira et al., 2020). QTLs on chromosomes 3, 5, 6, 7, 8, 10 and 11 also overlap with harvest, fruit abscission, width of ethylene peak, chlorophyll degradation and aroma QTLs (Galpaz et al., 2018; Obando-Ulloa et al., 2010; Pereira et al., 2020). Specifically, 92 QTLs for very diverse compounds converged into the QTL cluster on Chr08. These QTLs had high LOD scores and reproducibility in both 2015 and 2016

samples. In this region, *ETHQV8.1* has been recently described as a major regulator of climacteric ripening in melon (Pereira et al., 2020). Since 66 % of the Chr08 QTLs described in this work overlap with *ETHQV8.1*, including esters, aliphatic alcohols and phenylalanine derivatives, these compounds are most likely ethylene dependent. The region that does not contain *ETHQV8.1*, from 89-120 cM, included QTLs for ethyl esters and aldehydes. This region overlaps with many benzenoid, terpenoid and sulfur compounds QTLs identified in Galpaz et al. (2018), together with octanal and 3,6-nonadienal-(*Z,Z*) QTLs in Obando-Ulloa et al. (2010). Our results confirm that Chr08 is playing an important role in aroma production in our population.

5. Conclusions

Our work was focused on the genetics behind the biosynthesis of VOCs in melon to shed light to the complex metabolic pathways that affect its flavor. We evaluated two melon tissues at ripen stage, rind and flesh, since both affect consumer preferences in the market, but rind VOCs profile is still poorly known. In this study, we described the aroma profile in a PS x VED RIL population and its relationship with ripening behavior, mapping 166 QTLs to the melon genome. A QTL cluster on Chr08 was the most important contributor to volatile biosynthesis, mainly ethylene-related and overlapping with the major ripening QTL *ETHQV8.1* (Pereira et al., 2020). Moreover, QTL clusters identified in Ch02, Chr05, Chr06 and Chr11 contributed to decipher different VOCs synthesis pathways. These findings provide the ground for further fine-mapping projects and the functional validation of the candidate genes proposed related to aroma formation in melon.

CRediT authorship contribution statement

Carlos Mayobre: Methodology, Formal analysis, Writing - Original Draft. **Lara Pereira:** Methodology, Writing – Review & Editing. **Abdelali Eltahiri**: Methodology, Formal analysis. **Einat Bar**: Methodology. **Efraim Lewinsohn**: Writing – Review & Editing. **Jordi Garcia-Mas**: Conceptualization, Writing – Review & Editing, Supervision, Funding Acquisition. **Marta Pujol**: Conceptualization, Writing – Review & Editing, Supervision.

Declaration of Competing Interest

The authors declare that they have no known competing financial interests or personal relationships that could have appeared to influence the work reported in this paper.

Acknowledgements

This work was supported by the Spanish Ministry of Economy and Competitiveness grants AGL2015–64625-C2–1-R and RTI2018-097665-B-C2, the Severo Ochoa Programme for Centres of Excellence in R&D 2016-2010 (SEV-2015-0533), the CERCA Programme/Generalitat de Catalunya and 2017 SGR 1319 grant from the Generalitat de Catalunya to JGM. The authors also wish to thank the support of the Secretaria d'Universitats i Recerca del Departament d'Empresa i Coneixement de la Generalitat de Catalunya for having funded the 2019 FI_B 00124 project, and the co-funding of the European Social Fund (ESF – "*ESF is investing in your future"*) from the European Union. Special thanks to Fuensanta García for technical assistance in field and lab operations, as well as M. Bernardo for advice on data treatment and statistical analysis.

Appendix A. Supplementary Data

Supplementary Fig. S1. Boxplot showing the amount of VOCs according to their chemical group in rind (A) and flesh (B) samples of the parental lines (PS, VED) and the F1 (Hyb).

Supplementary Fig. S2. Principal component analysis (PCA) of the PS x VED RIL population volatile profile. The upper part represents rind PCAs for T3 (A), T4 (B) and T5 (C) subsets; the lower part represents flesh PCAs for T3 (D), T4 (E) and T5 (F) subsets. Different ellipses group climacteric lines (C), non-climacteric lines (NC) and "unstable-climacteric" lines (UC).

Supplementary Table S1. Average content of volatile compounds detected in the parental lines (PS, VED), the Hyb and in the RIL population for rind and flesh tissues.

Supplementary Table S2. Total VOC content according to the chemical classification and ripening classification of RILs.

Supplementary Table S3. VOC content in ng g-1 frozen tissue of each VOC in rind.

Supplementary Table S4. VOC content in ng g-1 frozen tissue of each VOC in flesh.

Supplementary Table S5. Positions of the QTLs detected in the PS x VED RIL population.

References

El-Sharkawy, I., Manríquez, D., Flores, F. B., Regad, F., Bouzayen, M., Latché, A., & Pech, J. C. (2005). Functional characterization of a melon alcohol acyl-transferase gene family involved in the biosynthesis of ester volatiles. Identification of the crucial role of a threonine residue for enzyme activity. *Plant Molecular Biology*, *59*(2), 345–362. https://doi.org/10.1007/s11103-005-8884-y

Esteras, C., Rambla, J. L., Sánchez, G., Granell, A., & Picó, M. B. (2020). Melon Genetic Resources Characterization for Rind Volatile Profile. *Agronomy*, *10*(1512). https://doi.org/10.3390/agronomy10101512

587 Esteras, C., Rambla, J. L., Sánchez, G., López-Gresa, M. P., González-Mas, M. C., Fernández-Trujillo, J. P., … Picó,
588 M. B. (2018). Fruit flesh volatile and carotenoid profile analysis within the Cucumis melo L. species reveals
589 unexploited variability for future genetic breeding. *Journal of the Science of Food and Agriculture*, *98*(10),
590 3915–3925. https://doi.org/10.1002/jsfa.8909

591 Flores, F., El Yahyaoui, F., de Billerbeck, G., Romojaro, F., Latché, A., Bouzayen, M., … Ambid, C. (2002). Role of
592 ethylene in the biosynthetic pathway of aliphatic ester aroma volatiles in Charentais Cantaloupe melons.
593 *Journal of Experimental Botany*, *53*(367), 201–206. https://doi.org/10.1093/jexbot/53.367.201

594 Freilich, S., Lev, S., Gonda, I., Reuveni, E., Portnoy, V., Oren, E., … Katzir, N. (2015). Systems approach for
595 exploring the intricate associations between sweetness, color and aroma in melon fruits. *BMC Plant*
596 *Biology*, *15*(1), 1–16. https://doi.org/10.1186/s12870-015-0449-x

597 Galpaz, N., Gonda, I., Shem-Tov, D., Barad, O., Tzuri, G., Lev, S., … Katzir, N. (2018). Deciphering genetic factors
598 that determine melon fruit-quality traits using RNA-Seq-based high-resolution QTL and eQTL mapping.
599 *Plant Journal*, *94*(1), 169–191. https://doi.org/10.1111/tpj.13838

600 Garcia-Mas, J., Benjak, A., Sanseverino, W., Bourgeois, M., Mir, G., Gonzalez, V. M., … Puigdomenech, P. (2012).
601 The genome of melon (Cucumis melo L.). *Proceedings of the National Academy of Sciences*, *109*(29),
602 11872–11877. https://doi.org/10.1073/pnas.1205415109

603 Goepfert, S., & Poirier, Y. (2007). β-Oxidation in fatty acid degradation and beyond. *Current Opinion in Plant*
604 *Biology*, *10*(3), 245–251. https://doi.org/10.1016/j.pbi.2007.04.007

605 Gonda, I., Bar, E., Portnoy, V., Lev, S., Burger, J., Schaffer, A. A., … Lewinsohn, E. (2010). Branched-chain and
606 aromatic amino acid catabolism into aroma volatiles in Cucumis melo L. fruit. *Journal of Experimental*
607 *Botany*, *61*(4), 1111–1123. https://doi.org/10.1093/jxb/erp390

608 Gonda, I., Burger, Y., Schaffer, A. A., Ibdah, M., Tadmor, Y., Katzir, N., … Lewinsohn, E. (2016). Biosynthesis and
609 perception of melon aroma. In *Biotechnology in Flavor Production* (pp. 281–305). Chichester, UK: John
610 Wiley & Sons, Ltd. https://doi.org/10.1002/9781118354056.ch11

611 Gonda, I., Davidovich-Rikanati, R., Bar, E., Lev, S., Jhirad, P., Meshulam, Y., … Lewinsohn, E. (2018). Differential
612 metabolism of L–phenylalanine in the formation of aromatic volatiles in melon (Cucumis melo L.) fruit.

Phytochemistry, *148*, 122–131. https://doi.org/10.1016/j.phytochem.2017.12.018

Gonda, I., Lev, S., Bar, E., Sikron, N., Portnoy, V., Davidovich-Rikanati, R., … Lewinsohn, E. (2013). Catabolism of l -methionine in the formation of sulfur and other volatiles in melon (Cucumis melo L.) fruit. *Plant Journal*, *74*(3), 458–472. https://doi.org/10.1111/tpj.12149

Ibdah, M., Azulay, Y., Portnoy, V., Wasserman, B., Bar, E., Meir, A., … Lewinsohn, E. (2006). Functional characterization of CmCCD1, a carotenoid cleavage dioxygenase from melon. *Phytochemistry*, *67*(15), 1579–1589. https://doi.org/10.1016/j.phytochem.2006.02.009

Ibdah, M., Chen, Y. T., Wilkerson, C. G., & Pichersky, E. (2009). An aldehyde oxidase in developing seeds of arabidopsis converts benzaldehyde to benzoic acid. *Plant Physiology*, *150*(1), 416–423. https://doi.org/10.1104/pp.109.135848

Jordán, M. J., Shaw, P. E., & Goodner, K. L. (2001). Volatile components in aqueous essence and fresh fruit of Cucumis melo cv. Athena (Muskmelon) by GC-MS and GC-O. *Journal of Agricultural and Food Chemistry*, *49*(12), 5929–5933. https://doi.org/10.1021/jf010954o

Kemp, T. R., Knavel, D. E., & Stoltz, L. P. (1972). cis-6-Nonenal: A flavor component of muskmelon fruit. *Phytochemistry*, *11*(11), 3321–3322. https://doi.org/10.1016/S0031-9422(00)86399-2

Lelievre, J.-M., Latche, A., Jones, B., Bouzayen, M., & Pech, J.-C. (1997). Ethylene and fruit ripening. *Physiologia Plantarum*, *101*, 727–739.

Li, Y., Qi, H., Jin, Y., Tian, X., Sui, L., & Qiu, Y. (2016). Role of ethylene in biosynthetic pathway of related-aroma volatiles derived from amino acids in oriental sweet melons (Cucumis melo var. makuwa Makino). *Scientia Horticulturae*, *201*, 24–35. https://doi.org/10.1016/j.scienta.2015.12.053

Lignou, S., Parker, J. K., Oruna-Concha, M. J., & Mottram, D. S. (2013). Flavour profiles of three novel acidic varieties of muskmelon (Cucumis melo L.). *Food Chemistry*, *139*(1–4), 1152–1160. https://doi.org/10.1016/j.foodchem.2013.01.068

Liu, S., Gao, P., Zhu, Q., Zhu, Z., Liu, H., Wang, X., … Luan, F. (2020). Resequencing of 297 melon accessions reveals the genomic history of improvement and loci related to fruit traits in melon. *Plant Biotechnology Journal*, 1–14. https://doi.org/10.1111/pbi.13434

639 Manríquez, D., El-Sharkawy, I., Flores, F. B., El-Yahyaoui, F., Regad, F., Bouzayen, M., … Pech, J. C. (2006). Two
640 highly divergent alcohol dehydrogenases of melon exhibit fruit ripening-specific expression and distinct
641 biochemical characteristics. *Plant Molecular Biology*, *61*(4–5), 675–685. https://doi.org/10.1007/s11103-
642 006-0040-9

643 Moing, A., Allwood, J. W., Aharoni, A., Baker, J., Beale, M. H., Ben-Dor, S., … Schaffer, A. A. (2020). Comparative
644 Metabolomics and Molecular Phylogenetics of Melon (Cucumis melo, Cucurbitaceae) Biodiversity.
645 *Metabolites*, *10*(3), 121. https://doi.org/10.3390/metabo10030121

646 Obando-Ulloa, J. M., Moreno, E., García-Mas, J., Nicolai, B., Lammertyn, J., Monforte, A. J., & Fernández-
647 Trujillo, J. P. (2008). Climacteric or non-climacteric behavior in melon fruit. 1. Aroma volatiles.
648 *Postharvest Biology and Technology*, *49*(1), 27–37. https://doi.org/10.1016/j.postharvbio.2007.11.004

649 Obando-Ulloa, J. M., Ruiz, J., Monforte, A. J., & Fernández-Trujillo, J. P. (2010). Aroma profile of a collection of
650 near-isogenic lines of melon (Cucumis melo L.). *Food Chemistry*, *118*(3), 815–822.
651 https://doi.org/10.1016/j.foodchem.2009.05.068

652 Pang, X., Guo, X., Qin, Z., Yao, Y., Hu, X., & Wu, J. (2012). Identification of aroma-active compounds in Jiashi
653 Muskmelon juice by GC-O-MS and OAV Calculation. *Journal of Agricultural and Food Chemistry*, *60*(17),
654 4179–4185. https://doi.org/10.1021/jf300149m

655 Pereira, L., Ruggieri, V., Pérez, S., Alexiou, K. G., Fernández, M., Jahrmann, T., … Garcia-Mas, J. (2018). QTL
656 mapping of melon fruit quality traits using a high-density GBS-based genetic map. *BMC Plant Biology*,
657 *18*(1), 1–17. https://doi.org/10.1186/s12870-018-1537-5

658 Pereira, L., Santo Domingo, M., Ruggieri, V., Argyris, J., Phillips, M. A., Zhao, G., … Garcia-Mas, J. (2020). Genetic
659 dissection of climacteric fruit ripening in a melon population segregating for ripening behavior.
660 *Horticulture Research*, *7*(1), 187. https://doi.org/10.1038/s41438-020-00411-z

661 Perry, P. L., Wang, Y., & Lin, J. (2009). Analysis of honeydew melon (Cucumis melo var. inodorus) flavour and
662 GC–MS/MS identification of (E,Z)-2,6-nonadienyl acetate. *Flavour and Fragrance Journal*, *24*, 341–347.

663 Pitrat, M. (2017). *Genetics and Genomics of Cucurbitaceae*. (R. Grumet, N. Katzir, & J. Garcia-Mas, Eds.) (1st ed.,
664 Vol. 20). Cham, Germany: Springer International Publishing. https://doi.org/10.1007/978-3-319-49332-9

665 Portnoy, V., Benyamini, Y., Bar, E., Harel-Beja, R., Gepstein, S., Giovannoni, J. J., … Katzir, N. (2008). The
666 molecular and biochemical basis for varietal variation in sesquiterpene content in melon (Cucumis melo
667 L.) rinds. *Plant Molecular Biology*, *66*(6), 647–661. https://doi.org/10.1007/s11103-008-9296-6

668 Schuster, J., Knill, T., Reichelt, M., Gershenzon, J., & Binder, S. (2006). BRANCHED-CHAIN AMINOTRANSFERASE4
669 is part of the chain elongation pathway in the biosynthesis of methionine-derived glucosinolates in
670 Arabidopsis. *Plant Cell*, *18*(10), 2664–2679. https://doi.org/10.1105/tpc.105.039339

671 Schwab, W., Davidovich-Rikanati, R., & Lewinsohn, E. (2008). Biosynthesis of plant-derived flavor compounds.
672 *The Plant Journal*, *54*(4), 712–732. https://doi.org/10.1111/j.1365-313X.2008.03446.x

673 Shalit, M., Katzir, N., Tadmor, Y., Larkov, O., Burger, Y., Shalekhet, F., … Lewinsohn, E. (2001). Acetyl-CoA:
674 Alcohol acetyltransferase activity and aroma formation in ripening melon fruits. *Journal of Agricultural*
675 *and Food Chemistry*, *49*(2), 794–799. https://doi.org/10.1021/jf001075p

676 Shi, J., Wu, H., Xiong, M., Chen, Y., Chen, J., Zhou, B., … Huang, Y. (2020). Comparative analysis of volatile
677 compounds in thirty nine melon cultivars by headspace solid-phase microextraction and gas
678 chromatography-mass spectrometry. *Food Chemistry*, *316*(January), 126342.
679 https://doi.org/10.1016/j.foodchem.2020.126342

680 Tang, Y., Zhang, C., Cao, S., Wang, X., & Qi, H. (2015). The effect of CmLOXs on the production of volatile
681 organic compounds in four aroma types of melon (Cucumis melo). *PLoS ONE*, *10*(11), 1–18.
682 https://doi.org/10.1371/journal.pone.0143567

683 Tzuri, G., Zhou, X., Chayut, N., Yuan, H., Portnoy, V., Meir, A., … Tadmor, Y. (2015). A “golden” SNP in CmOr
684 governs the fruit flesh color of melon (Cucumis melo). *Plant Journal*, *82*(2), 267–279.
685 https://doi.org/10.1111/tpj.12814

686 Van Bel, M., Diels, T., Vancaester, E., Kreft, L., Botzki, A., Van De Peer, Y., … Vandepoele, K. (2018). PLAZA 4.0:
687 An integrative resource for functional, evolutionary and comparative plant genomics. *Nucleic Acids*
688 *Research*, *46*(D1), D1190–D1196. https://doi.org/10.1093/nar/gkx1002

689 Vogel, J. T., Tan, B. C., McCarty, D. R., & Klee, H. J. (2008). The carotenoid cleavage dioxygenase 1 enzyme has
690 broad substrate specificity, cleaving multiple carotenoids at two different bond positions. *Journal of*

691 *Biological Chemistry*, *283*(17), 11364–11373. https://doi.org/10.1074/jbc.M710106200

692 Wyllie, S. G., Leach, D. N., Wang, Y., & Shewfelt, R. L. (1994). Sulfur Volatiles in Cucumis melo cv. Makdimon
693 (Muskmelon) Aroma. In *Sulfur Compounds in Foods* (pp. 36–48). https://doi.org/10.1021/bk-1994-
694 0564.ch004

695 Wyllie, S. G., Leach, D. N., Wang, Y., & Shewfelt, R. L. (1995). Key Aroma Compounds in Melons. In *Fruit Flavors*
696 (pp. 248–257). https://doi.org/10.1021/bk-1995-0596.ch022

697 Yahyaoui, F. E. L., Wongs-Aree, C., Latché, A., Hackett, R., Grierson, D., & Pech, J. C. (2002). Molecular and
698 biochemical characteristics of a gene encoding an alcohol acyl-transferase involved in the generation of
699 aroma volatile esters during melon ripening. *European Journal of Biochemistry*, *269*(9), 2359–2366.
700 https://doi.org/10.1046/j.1432-1033.2002.02892.x

701 Yano, R., Nonaka, S., & Ezura, H. (2018). Melonet-DB, a Grand RNA-Seq Gene Expression Atlas in Melon
702 (Cucumis melo L.). *Plant and Cell Physiology*, *59*(1), e4(1-15). https://doi.org/10.1093/pcp/pcx193

703 Zhao, G., Lian, Q., Zhang, Z., Fu, Q., He, Y., Ma, S., … Huang, S. (2019). A comprehensive genome variation map
704 of melon identifies multiple domestication events and loci influencing agronomic traits. *Nature Genetics*,
705 *51*(11), 1607–1615. https://doi.org/10.1038/s41588-019-0522-8

706

707

708

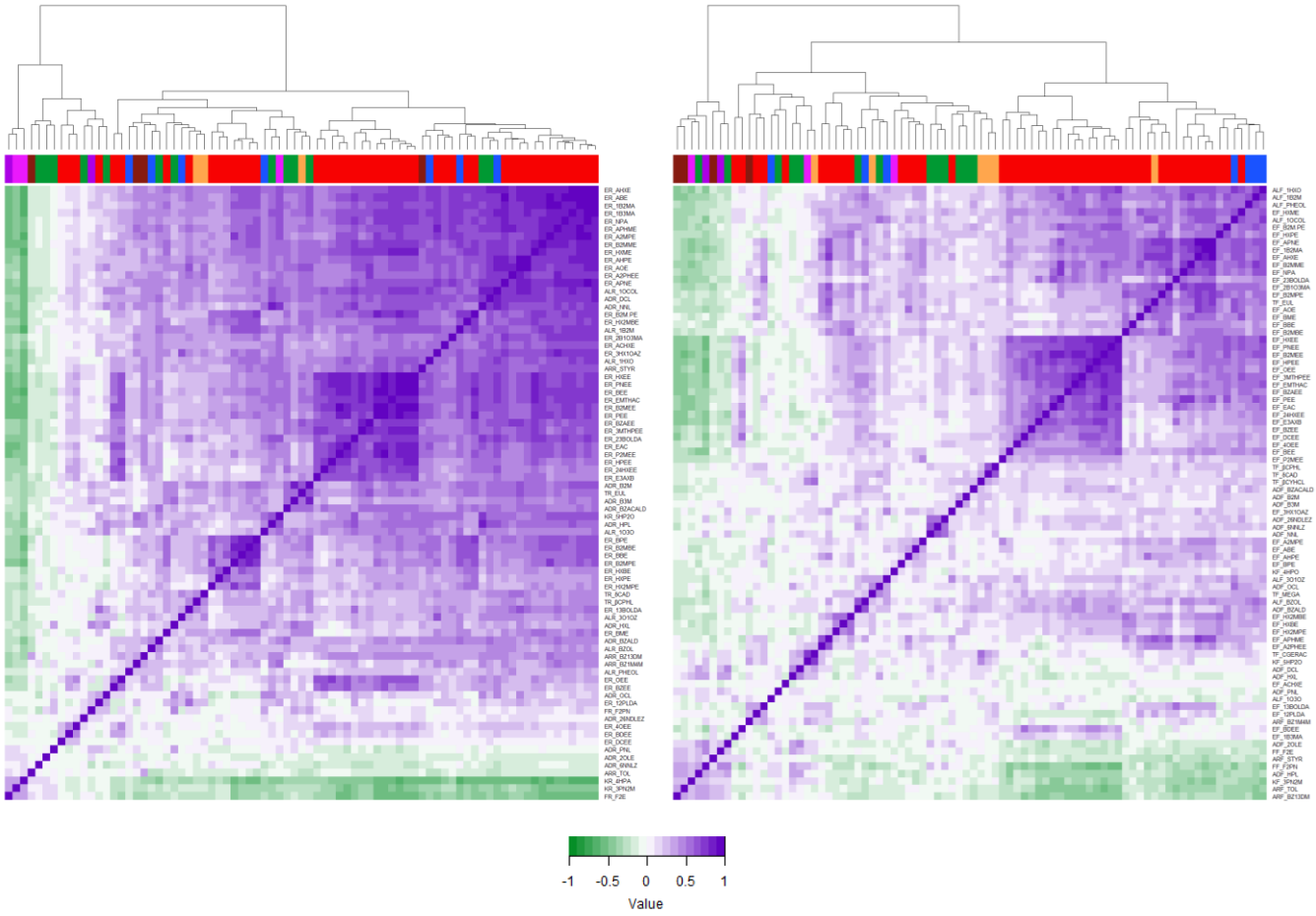

Fig. 1. Heatmap and dendrogram showing the correlation matrix by the Spearman's coefficient between VOCs in the RIL population for rind (A) and flesh (B).

709

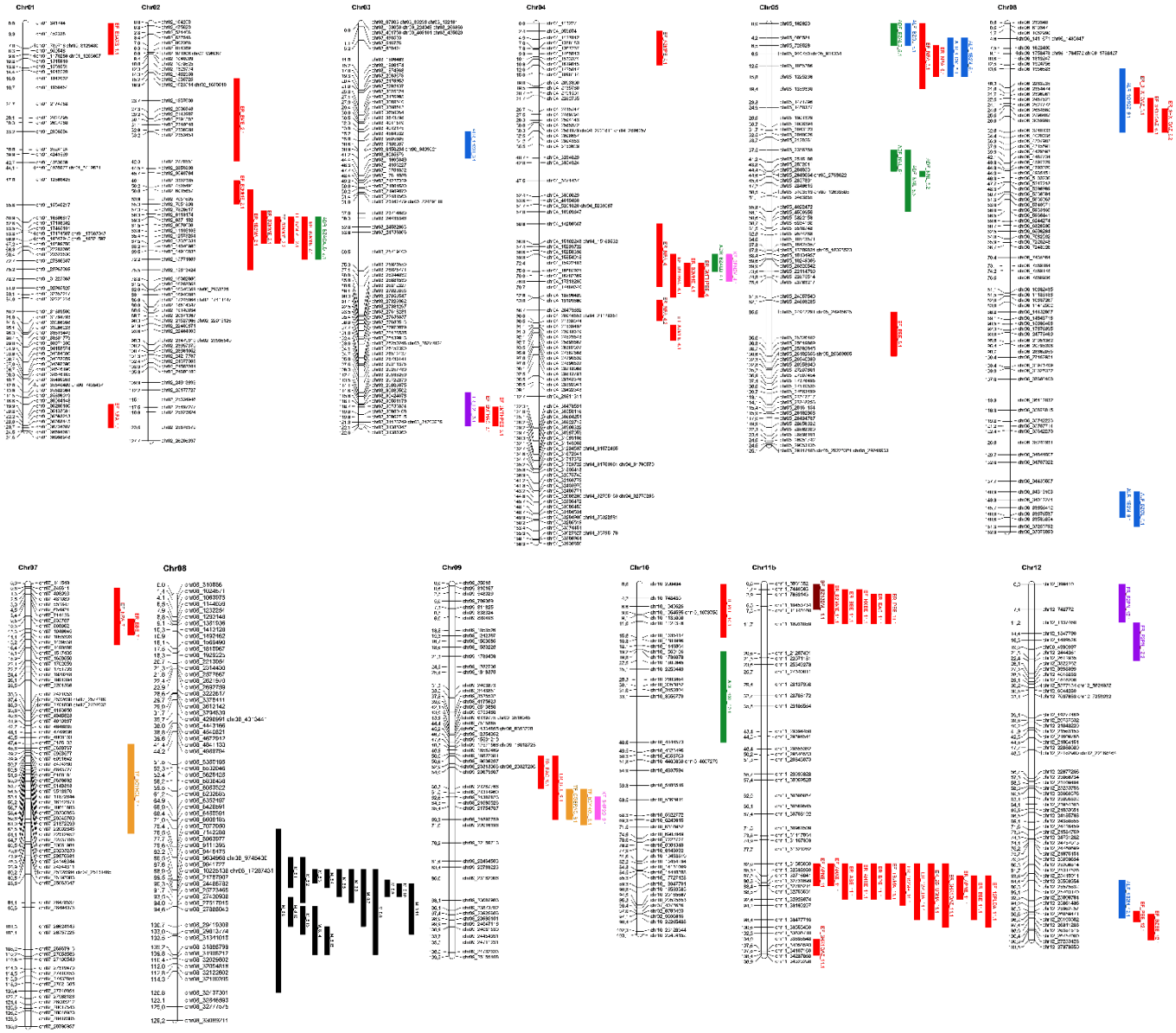

Fig. 2. Genetic map showing QTLs found in rind and flesh. QTLs for esters (red), alcohols (blue), aldehydes (green), terpenes (orange), benzenoids (brown), ketones (pink) and furans (purple) were represented selecting LOD-1 as upper and lower limit. Black QTLs represent merged (M) QTLs coincident for several compounds.

710

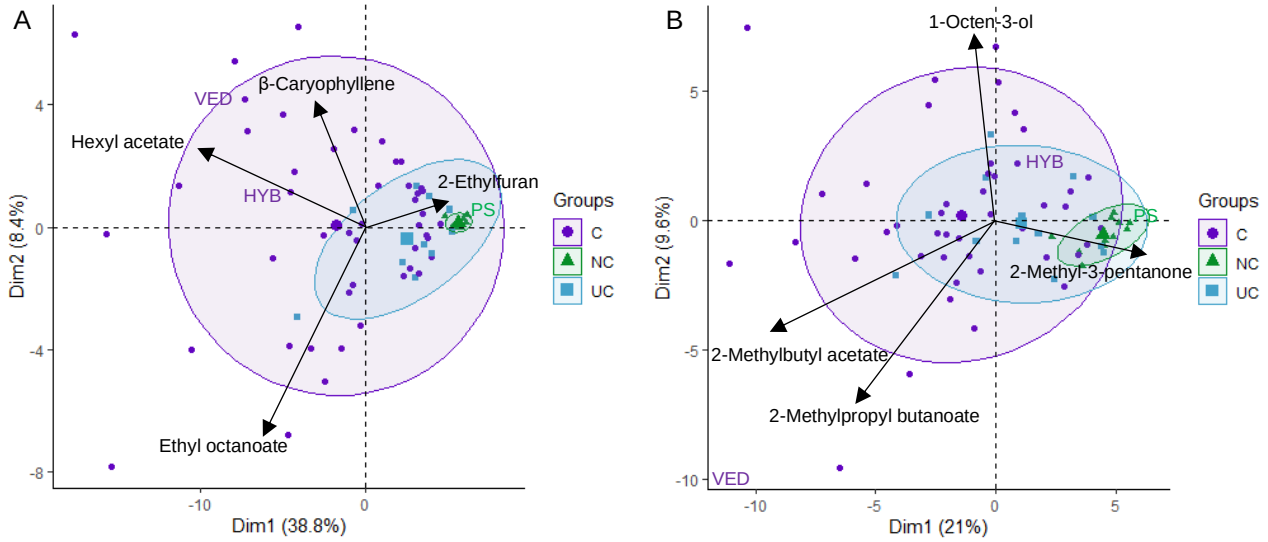

Fig. 3. Principal component analysis (PCA) of the PS x VED RIL population volatile profile in rind (A) and flesh (B). Different ellipses group climacteric lines (C), non-climacteric lines (NC) and "unstable-climacteric" lines (UC). The arrows represent the VOCs with the most positive and negative effect for the two principal components.

711

712

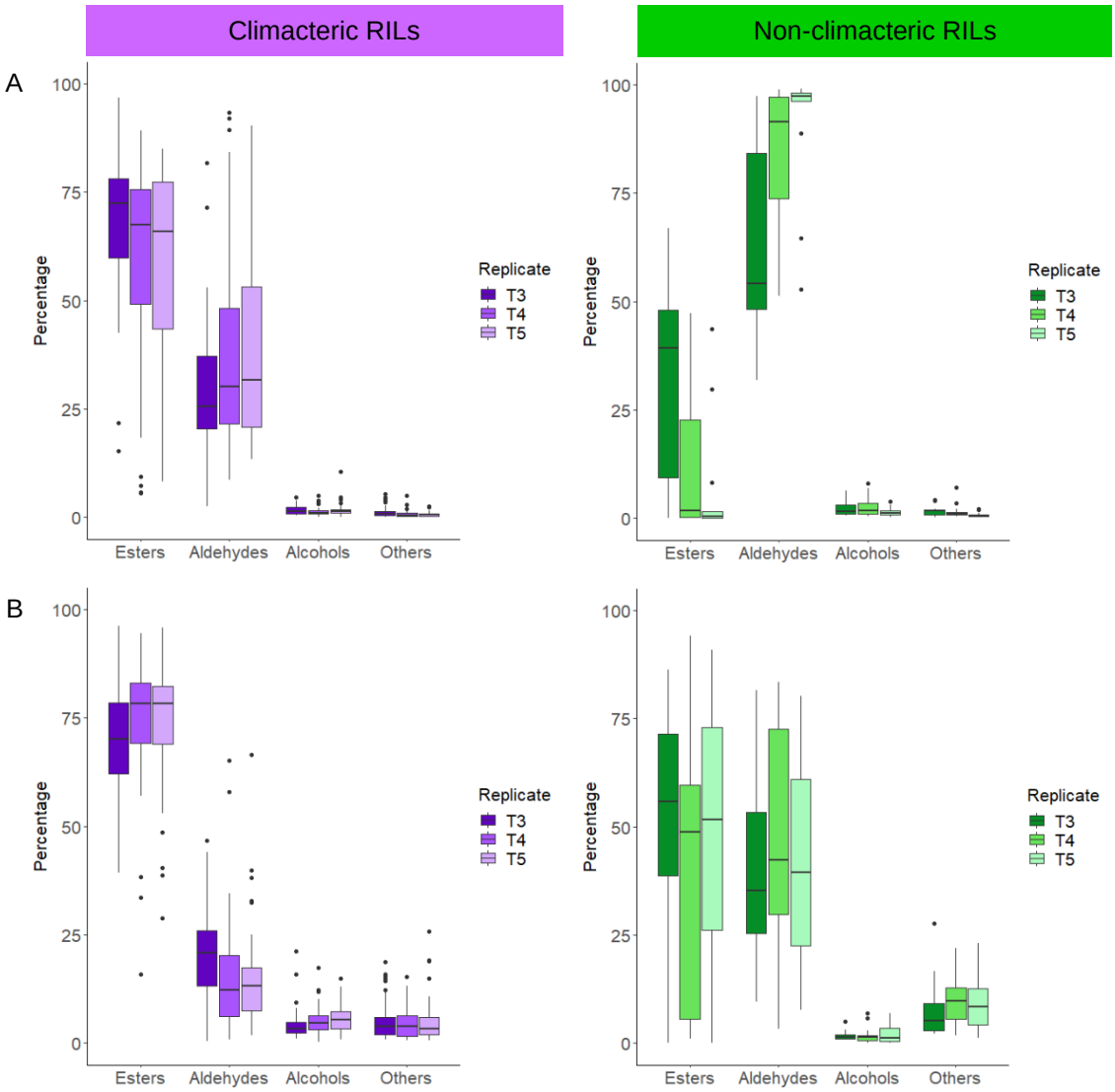

Fig. 4. Percentage of VOCs in RILs according to their chemistry, in rind (A) and flesh (B). Data from three subsets with plants performed in 2015 (T3) and 2016 (T4, T5) are represented.

713

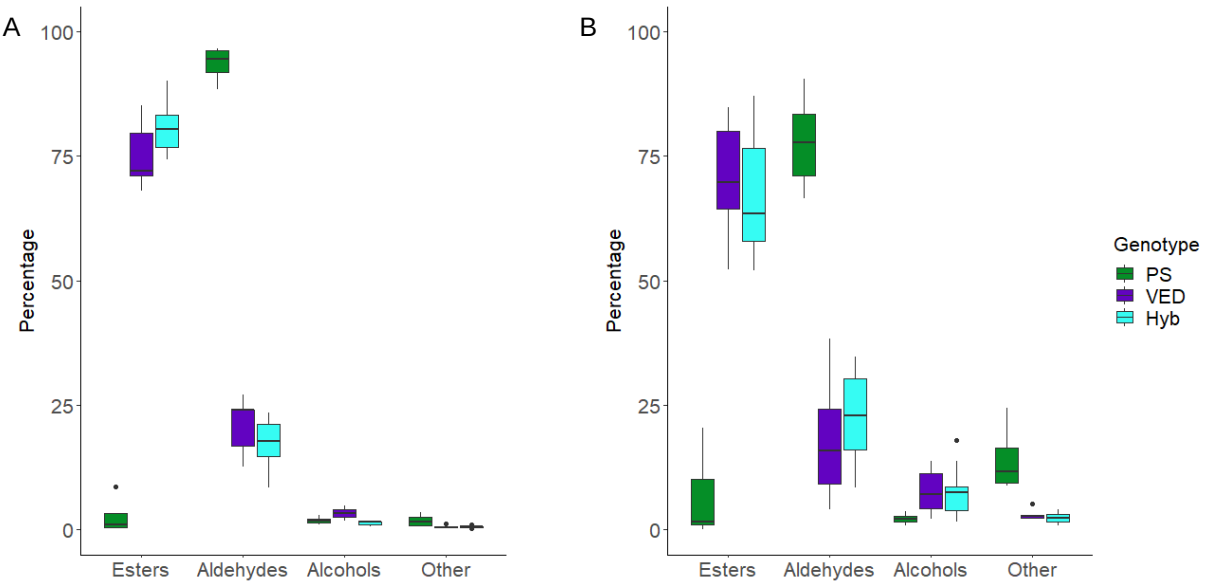

Supplementary Fig. S1. Boxplot showing the amount of VOCs according to their chemical group in rind (A) and flesh (B) samples of the parental lines (PS, VED) and the F1 (Hyb).

714

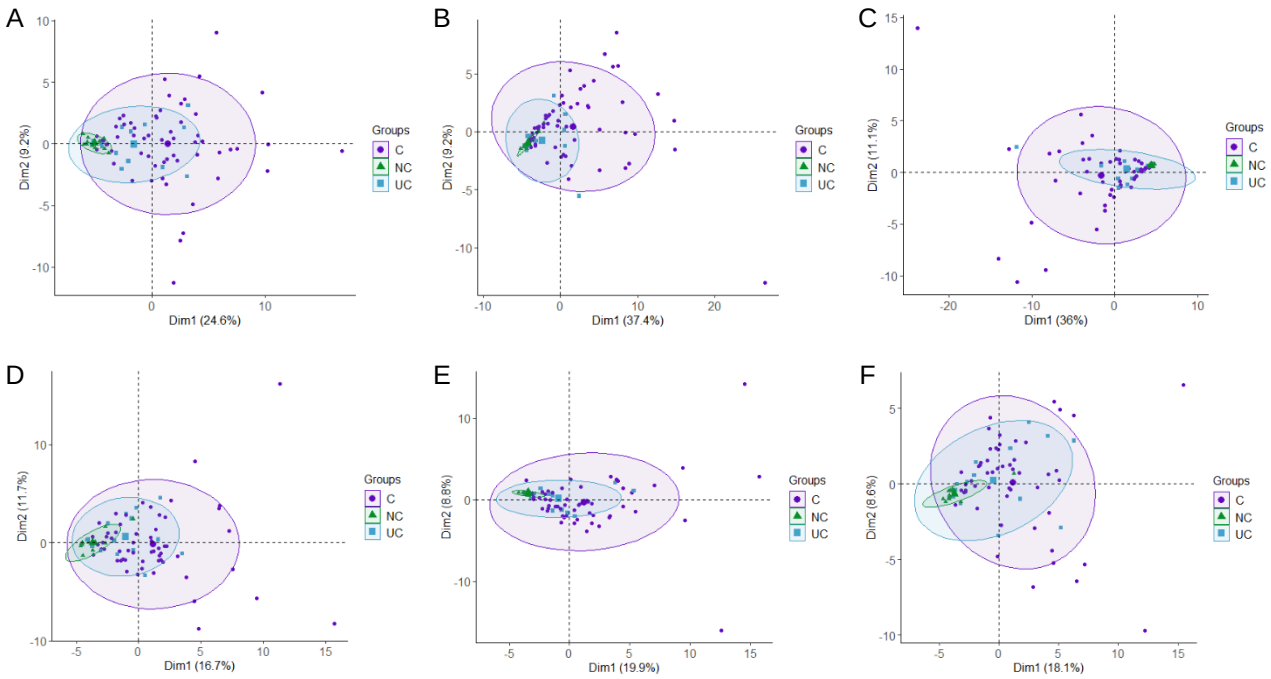

Supplementary Fig. S2. Principal component analysis (PCA) of the PS x VED RIL population volatile profile. The upper part represents rind PCAs for T3 (A), T4 (B) and T5 (C) subsets; the lower part represents flesh PCAs for T3 (D), T4 (E) and T5 (F) subsets. Different ellipses group climacteric lines (C), non-climacteric lines (NC) and "unstable-climacteric" lines (UC).